

PARTICLE SYSTEMS ARISING FROM AN ANTI-FERROMAGNETIC ISING MODEL

SUNIL CHHITA

ABSTRACT. We study a low temperature anisotropic anti-ferromagnetic 2D Ising model through the guise of a certain dimer model. This model has a bijection with a one-dimensional particle system equipped with creation and annihilation. In the thermodynamic limit, we determine the explicit phase diagrams as functions of temperature and anisotropy. Two values of the anisotropy are of particular interest - the ‘critical’ value and the ‘independent’ value. At independence, the particle system has the same distribution as the two colored noisy voter model. Its limiting measure under a natural scaling window is the Continuum Noisy Voter Model. At criticality, the distribution of particles on a given horizontal line, is a Pfaffian point process whose kernel in the scaling window can be written explicitly in terms of Bessel functions. We also show that ‘macroscopic’ creations form a Poisson point process.

1. INTRODUCTION

1.1. History. The dimer model is a two-dimensional exactly solvable model, which can be described in the following manner. A dimer configuration for a planar graph is a subset of edges in which each vertex is covered exactly once by an edge. The dimer model is a probability measure on the set of all dimer configurations of the underlying planar graph. Weights can be applied to the edges so that specific edges have higher or lower probabilities of being observed.

The dimer model was initially introduced in [Kas61]. [Fis66] noticed the correspondence between the dimer model and the two-dimensional Ising Model. Since its introduction, the dimer model has been studied extensively and a vast variety of techniques have been developed using many areas of mathematics. Much of this work was completed by R. Kenyon and A. Okounkov during the late 90’s and 00’s (for an excellent survey of their body of results, see [Ken09]). The dimer model is a rather unique statistical mechanical model - not only can a partition function be easily found but by [Ken97], local statistics can be computed.

Dimer models on non-bipartite lattices are fundamentally different to dimer models on bipartite lattices. For instance, we can define a height function if and only if the underlying lattice is bipartite (see [Ken00]), which leads to connections with random surfaces ([She05]). Recently, there has been renewed interest in the study of dimer coverings on non-bipartite lattices. In particular, [BdT08] have shown that some of the machinery for the dimer model on bipartite lattices transfers to non-bipartite lattices.

1.2. The Dimer model on the Fisher lattice. This paper focuses on a dimer model on a particular non-bipartite lattice, called the Fisher Lattice, introduced in [Fis66]. The Fisher lattice consists of a honeycomb lattice with a triangle decoration at each vertex as depicted in Figure 1. All vertical edges are referred to as **a** edges. All edges outside the triangle

Key words and phrases. Dimer Model, Antiferromagnetic Ising Model, Noisy Voter Model, Continuum Noisy Voter Model, Scaling Windows, Pfaffian Point process.

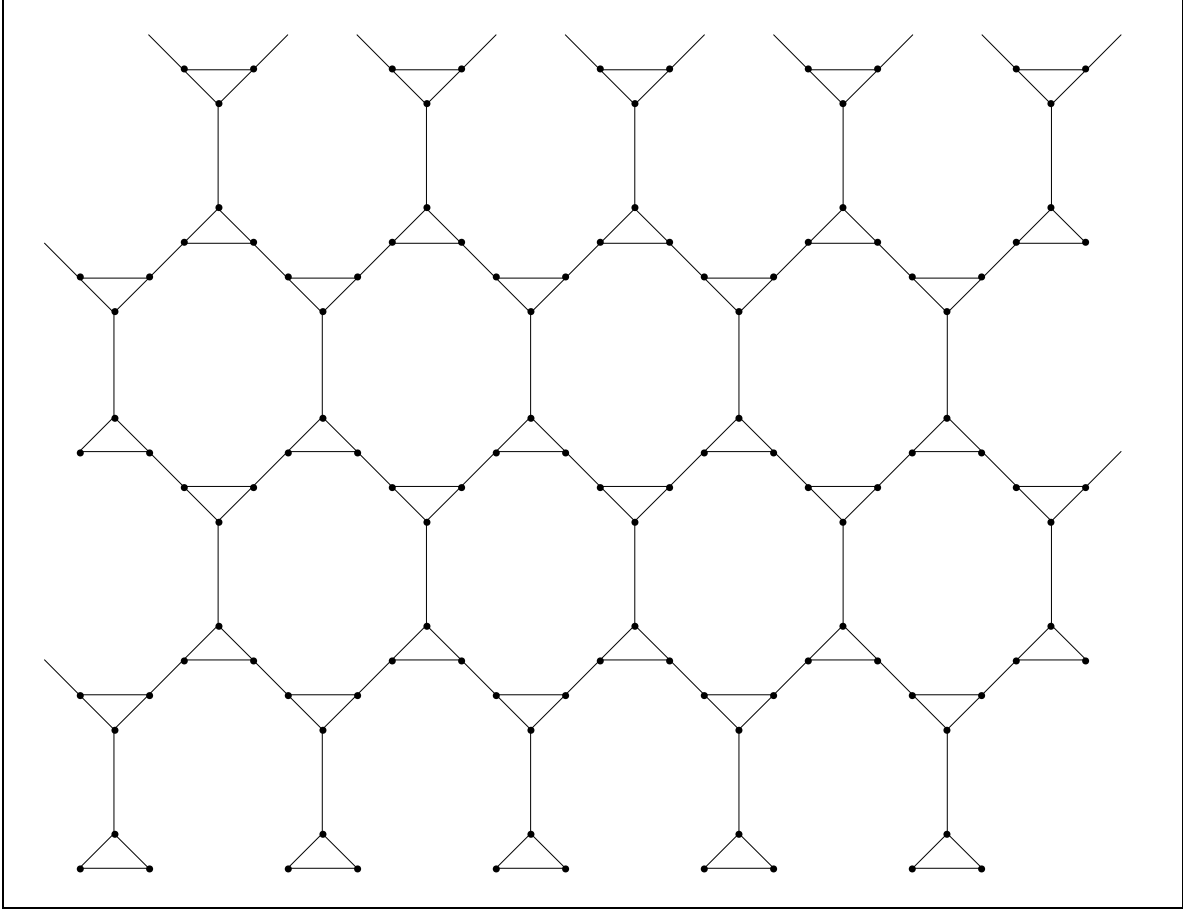


Figure 1: The Fisher Lattice

decoration which are not vertical are referred to as **b** edges. We give weight a to the **a** edges, weight b to the **b** edges and weight 1 to the remaining edges.

Let G denote the Fisher lattice on the plane. Define the toroidal graph G_n to be the quotient $G/n\mathbb{Z}^2$ where the action $n\mathbb{Z}^2$ are translations by $(n, 0)$ and $(0, n)$ (horizontal and vertical translations). Let $\mathcal{M}(G_n)$ denote the set of all dimer coverings of G_n . We can define a probability measure μ_n for $M \in \mathcal{M}(G_n)$ so that the probability of M is proportional to the product of all the edge weights; that is,

$$(1.1) \quad \mu_n(M) = \frac{a^{N_a} b^{N_b}}{Z(G_n)}$$

where $N_a = N_a(M)$ and $N_b = N_b(M)$ are the number of dimers covering **a** and **b** edges for the dimer covering M and, $Z(G_n)$ is the partition function: $Z(G_n) = \sum_{M \in \mathcal{M}(G_n)} a^{N_a} b^{N_b}$.

1.3. Anti-ferromagnetic Ising model and Setup. Here, we describe the one-to-two correspondence between the dimer model on the Fisher lattice and an anisotropic anti-ferromagnetic 2D Ising model (explained below), as described in [Fis66].

Let Λ_n represent the faces of the dodecahedrons in G_n . Let $\Omega := \{-1, +1\}^{\Lambda_n}$ and let $\sigma_x \in \{-1, 1\}$ denote the spin at $x \in \Lambda_n$. For $\sigma \in \Omega$, define the Hamiltonian by

$$(1.2) \quad H(\sigma) = \sum_{v \in \Lambda} \sum_{v \sim w} J_{v,w} \frac{\sigma_v \sigma_w + 1}{2}$$

where $v \sim w$ means that v and w are nearest neighbors and $J_{v,w}$ is the *interaction* term between the faces v and w . For $\sigma \in \Omega$, define the probability measure,

$$(1.3) \quad \nu_n(\sigma) = \frac{e^{-H(\sigma)}}{Z(\Lambda_n)}$$

where $Z(\Lambda_n)$ is the partition function: $Z(\Lambda_n) = \sum_{\sigma \in \Omega} e^{-H(\sigma)}$. The above probability measure is called the Ising model.

The correspondence between the Ising model and dimer model can be seen in Figure 2 and is as follows. Faces sharing an edge have the same spin if there is a dimer covering the shared edge. Otherwise, the faces have opposite spins.

$$(1.4) \quad J_{v,w} = \begin{cases} \log a & w \sim v \text{ and } vw \text{ is an } \mathbf{a} \text{ edge} \\ \log b & w \sim v \text{ and } vw \text{ is a } \mathbf{b} \text{ edge,} \end{cases}$$

where vw is the shared edge (on the Fisher lattice) between the faces w and v . It is clear that

Lemma 1.

$$(1.5) \quad 2Z(G_n) = Z(\Lambda_n)$$

We choose $a = x$ and $b = ux$ where $x < 1$ and $u \in (0, 1)$. As $u < 1/x$ then $J_{v,w} < 0$ for $v \sim w$, which means that adjacent sites have a high probability of having opposite spins. This is called an anti-ferromagnetic interaction. Furthermore, $J_{v,w}$ depends on the direction of the edge between the sites v and w . This is called an anisotropic interaction. The parameter x controls the temperature (because the temperature is equal to $1/(\log(1/x))$). The anisotropy is controlled by the parameter u . We shall sometimes refer to u as the anisotropy.

Finally, we heuristically describe the concept of *thermodynamic limit*. As previously mentioned, dimer coverings of the torus G_n give a probability measure μ_n . The *thermodynamic limit* is the measure, $\mu = \mu(u, x) = \lim_{n \rightarrow \infty} \mu_n$, i.e. the limiting measure obtained when the system size is sent to infinity. More information on the thermodynamic limit can be found in Section 2.

1.4. The particle model. By considering the horizontal axis as space and the vertical axis as time, the dimer model, μ , is in bijection with a one-dimensional particle system called the *particle model*. This is a probability measure on the set of all possible bi-infinite lines, finite loops and pairs of infinite lines with the same starting points on the diagonal grid.

For each dimer configuration there is a realization of the particle model, and vice versa, chosen with the same probability. An example of the correspondence can be seen in Figure 3. Each realization of the particle model is obtained from a dimer covering of the Fisher lattice by collapsing the \mathbf{a} edges and the triangle decoration. This leaves a diagonal grid, where each dimer covering a \mathbf{b} edge in the dimer model can be thought of as a trajectory of a particle in the particle model. By the structure of the underlying dimer model, particles can be created or annihilated in pairs and there is no branching or coalescence of particles. The above construction shows that the particle model is in bijection with dimer model of the Fisher lattice.

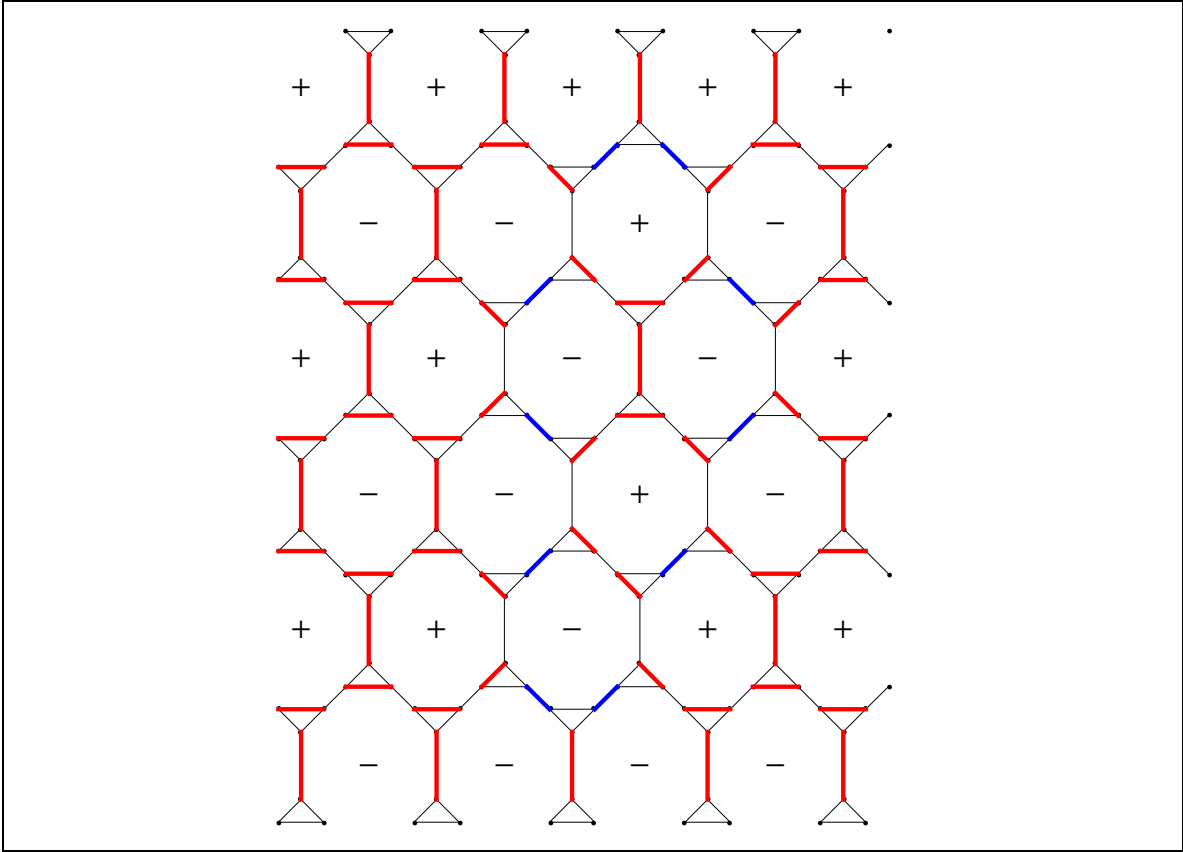


Figure 2: The correspondence between the Ising model and dimer coverings on the Fisher lattice. The blue edges represent dimers covering **b** edges. The red edges are dimers covering the decoration and **a** edges. The ‘+’ and ‘-’ are spins in the corresponding Ising model.

We say that a *singularity* occurs when there are no dimers covering any edges at a triangle decoration. A singularity is called a *creation (annihilation)* if the **a** edge is below (above) the triangle decoration. We use the terminology creation (annihilation) because that singularity is a creation (annihilation) of two particles in the particle model. We adopt the convention that a particle is located at a point if there is no dimer covering the corresponding **a** edge.

1.5. Scaling Limits and Scaling Windows. Here, we heuristically describe the concepts of scaling limit and scaling window. More specific information regarding scaling windows for the dimer model on the Fisher lattice, can be found in Section 2.

The scaling limit of grid-based models is a subtle concept and we make no attempt to define it rigorously. Informally, we can think of the *scaling limit* as the limiting measure of some measure when sending the lattice spacing to zero. For a two-dimensional lattice (e.g. \mathbb{Z}^2), the vertical and horizontal lattice spacings need not be sent to zero at the same rate. For example, Donsker’s scaling of a simple symmetric one dimensional random walk has different vertical and horizontal scalings (by considering the trajectory of the walk on a diagonal grid). For many statistical models, scaling limits are only non-trivial provided that the model is at *criticality*. In this context, criticality refers to the correlation length, defined in (1.16), being infinite. See [FFS92] for discussions regarding criticality and [Sch00] for the underlying philosophy of scaling limits of statistical mechanical models.

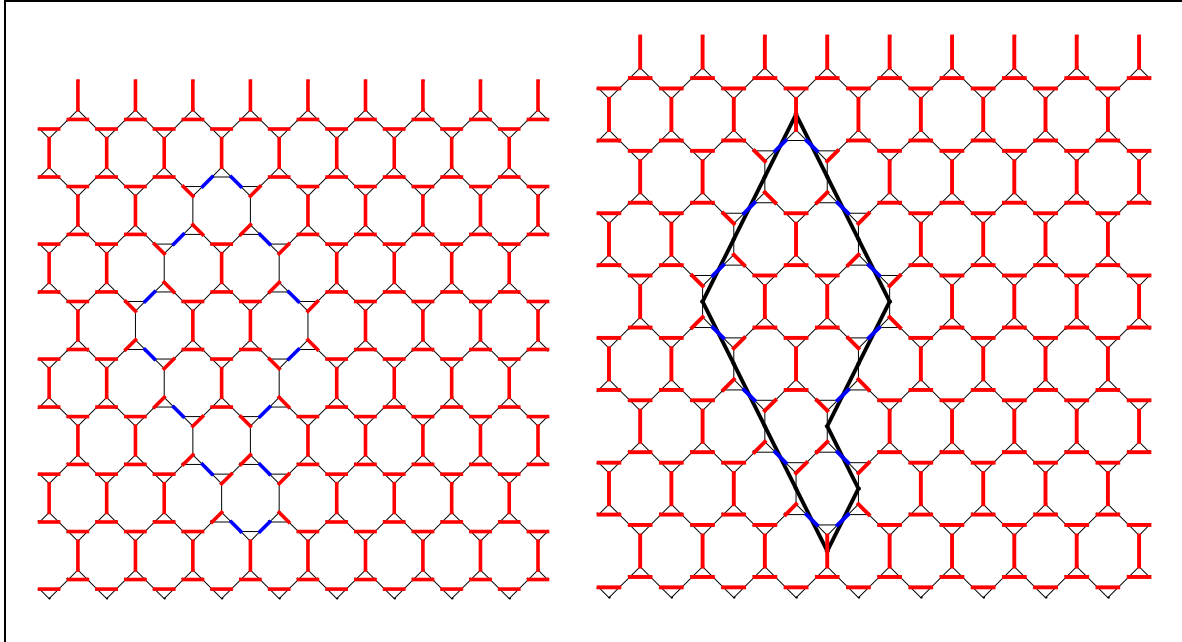


Figure 3: A dimer configuration with its corresponding particle model

The concept of the scaling window is equally as subtle as the concept of the scaling limit. In this case, we do provide a watertight mathematical definition for the particle model (see Section 2) as it is one of the main aspects of this paper. Roughly speaking, a *scaling window* is the limiting measure of some measure when sending the lattice spacing to zero while simultaneously sending a certain parameter to zero. Similar to a scaling limit, the choice of the re-scaling is important in guaranteeing non-trivial behavior. This choice usually involves having constant density of some observable in the scaling window. For example, we could choose the scaling window so that the density of particles is constant along any arbitrary horizontal line.

Contrary to the scaling limit, the scaling window preserves microscopic behavior of the discrete model, which means that the scaling window is non-trivial regardless of whether the model is critical. In particular, the scaling window of a critical model is still critical. Indeed, the scaling window of a critical model can only be achieved if the model has two (or more) parameters. This is a consequence of criticality being a relationship between the available parameters.

In this paper, all scaling windows are taken with respect to the parameter x . We will only consider scaling windows after the thermodynamic limit has been taken. We will only consider scaling windows of the particle model and the distributions of the particles on an arbitrary horizontal line. We use the following terminology for scaling windows: For $\alpha, \beta > 0$, the scaling window (x^α, x^β) of a measure is the limiting measure obtained when sending a box of lattice points of size $(1/x^\alpha, 1/x^\beta)$ to a box in the continuum of size $(1, 1)$, when $x \rightarrow 0$.

We can now state and explain our main results. First, we consider the behavior in the thermodynamic limit and in particular, highlight the behavior at low temperature (i.e. which means x is small) for different values of the anisotropy, u . We can then focus on taking scaling windows for different values of the anisotropy parameter.

1.6. Statement of the results.

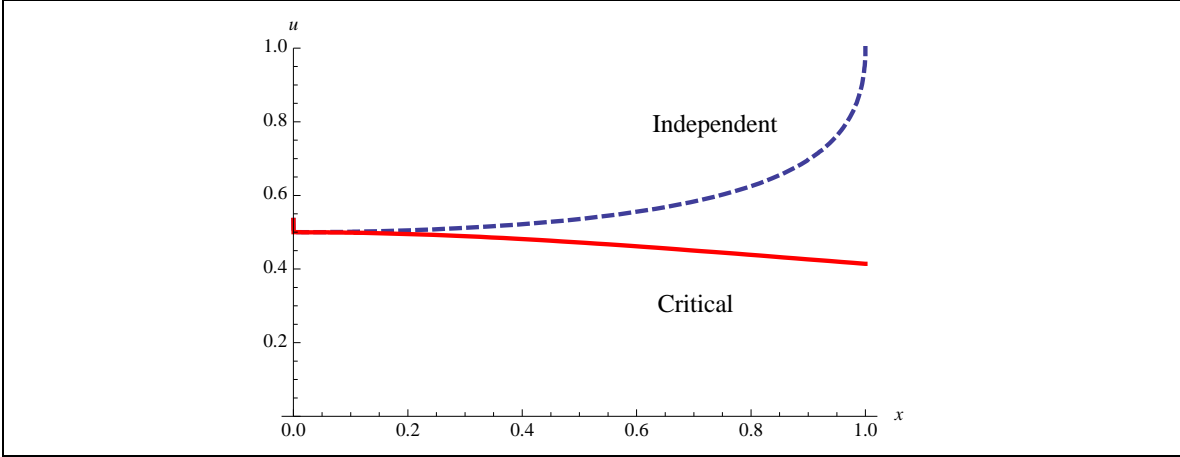


Figure 4: The Phase Diagram in terms of u and x . The solid line represents criticality, where the partition function is non-analytic. The dashed line represents independence.

Recall that $\mu = \mu(x, u)$ is the thermodynamic limit. Define $u_c := (-1 + \sqrt{1 + x^2})/x^2$, $u_i := (1 - \sqrt{1 - x^2})/x^2$, $\mu_0 = \lim_{x \rightarrow 0} \mu(u, x)$ and $\mathbb{P}_\mu(\cdot)$ denote the probability of the event \cdot under μ .

Under μ , Theorem 5 gives an explicit formula for the expected number of **a**, **b** edges and creations per fundamental domain for $x \in (0, 1)$ and $u \in (0, 1)$. Essentially, each expectation can be written as a linear combination of elliptic integrals, with the exact expression dependent on whether $u < u_c$, $u = u_c$ or $u > u_c$. By considering a low temperature expansion, then

Theorem 1. *Under μ_0 ,*

$$(1.6) \quad \mathbb{P}_{\mu_0}(\text{particle}) = \begin{cases} 0 & \text{if } u \leq \frac{1}{2} \\ 2 - \frac{2}{\pi} \arccos\left(-\frac{1}{2u}\right) & \text{if } u > \frac{1}{2} \end{cases}$$

and

$$(1.7) \quad \mathbb{P}_{\mu_0}(\text{creation}) = 0.$$

In this limit, there is a phase transition at $u = 1/2$. As there are no creations (or annihilations), then particles form non-intersecting lattice paths for $u > 1/2$. The above behavior is *only* exhibited under μ_0 .

We can now consider the phase behavior for $u < u_c$ chosen independently of x which leads to choosing a natural re-scaling for the scaling window of the particle model:

Theorem 2. *For $u < u_c$ chosen independently of x , the scaling window (x, x) of the particle model is a Poisson Point process with intensity $u^2 \left(1/\sqrt{1 - 4u^2} - 1\right)$.*

Under $\mu = \mu(u_i, x)$ with $x > 0$, the locations of particles in the particle model along a horizontal line are distributed according to an i.i.d. Bernoulli with probability $x/(1 + x)$. Each trajectory of a particle is independent of the trajectories of other particles and along each horizontal line, creations are i.i.d. Bernoulli with probability cx^2 (where c is some constant). This leads to the noisy voter model interpretation of the particle model which is described below.

The (non-noisy) voter model on \mathbb{Z} with two colors is a time dependent probability measure with state space $\{R, B\}^{\mathbb{Z}}$. The update of each site is given by randomly choosing the color of a neighboring site (see [Lig85]). The noisy voter model of two colors with noise p was introduced in [GM95]. Each site chooses at random the color of a neighboring site with probability $1 - p$ or flips its color with probability p . [FINR06] constructed the scaling window (x, x^2) of the noisy voter model with noise cx^2 (c is a constant) and called it the Continuum Noisy Voter Model (CNVM). This construction relies on using the Brownian Web (see [FINR04]) and the dual Brownian Web. The correspondence for the particle model at the special case when $u = u_i$ and the noisy voter model is as follows. The paths in the particle model are shown, in Section 6, to represent the boundaries between the two colors in the noisy voter model. It is not surprising that

Theorem 3. *At $u = u_i$, the particle model has the same distribution as the color boundaries of the two color noisy voter model. In the scaling window (x, x^2) , the particle model converges in distribution to the CNVM.*

We can now consider the behavior for $u_\gamma := (1 - \sqrt{1 - x^2\gamma})/(\gamma x^2) = 1/2 + \gamma x^2/8 + O(x^4)$. Notice that $u_{-1} = u_c$ and $u_1 = u_i$. We find the stationary measure for particle locations at time $t \in \mathbb{R}$ in the scaling window (x, x^2) .

Theorem 4. *For $u = u_\gamma$ but $\gamma \neq 1$, in the scaling window (x, x^2) the distributions of the particles along an arbitrary horizontal line are given by a Pfaffian point process, \mathbb{P}_0^γ , with kernel*

$$(1.8) \quad M_{\gamma, x}^{res}(y, y) = \begin{pmatrix} 0 & e(\gamma) \\ -e(\gamma) & 0 \end{pmatrix}$$

for $y \in \mathbb{R}$ and for $y_1 \in \mathbb{R}$ and for $y_2 \in \mathbb{R}$ with $y_1 < y_2$

$$(1.9) \quad M_{\gamma, x}^{res}(y_1, y_2) = \begin{pmatrix} -E_1^\gamma(y_1 - y_2) & -E_2^\gamma(|y_1 - y_2|) \\ E_2^\gamma(|y_1 - y_2|) & E_1^\gamma(|y_1 - y_2|) \end{pmatrix}.$$

where for $e_1(\gamma) = 2 + \sqrt{2(1 - \gamma)}$, $e_2(\gamma) = (2 - \sqrt{2(1 - \gamma)})\mathbb{I}_{\gamma > -1} + (-2 + \sqrt{2(1 - \gamma)})\mathbb{I}_{\gamma < -1}$ and $\alpha > 0$, we have

$$(1.10) \quad e(\gamma) = \frac{1}{\pi i} \int_{e_2(\gamma)}^{e_1(\gamma)} \frac{2 - 2\gamma + p^2}{2\sqrt{4 + 8\gamma + 4\gamma^2 - 12p^2 + 4\gamma p^2 + p^4}} dp,$$

$$(1.11) \quad E_1^\gamma(\alpha) = -\frac{1}{\pi i} \int_{e_2(\gamma)}^{e_1(\gamma)} \frac{2pe^{-\alpha p}}{\sqrt{4 + 8\gamma + 4\gamma^2 - 12p^2 + 4\gamma p^2 + p^4}} dp$$

and

$$(1.12) \quad E_2^\gamma(\alpha) = \frac{1}{\pi i} \int_{e_2(\gamma)}^{e_1(\gamma)} \frac{(-2 - 2\gamma - p^2)e^{-\alpha p}}{2\sqrt{4 + 8\gamma + 4\gamma^2 - 12p^2 + 4\gamma p^2 + p^4}} dp.$$

In the special case when $\gamma = -1$, $e(-1) = 2/\pi$,

$$(1.13) \quad E_1^{-1}(\alpha) = B_I(0, 4\alpha) - S_L(0, 4\alpha) = \frac{1}{\pi} \int_0^\pi e^{-4\alpha \sin \theta} d\theta$$

and

$$(1.14) \quad E_2^{-1}(\alpha) = S_L(-1, 4\alpha) - B_I(0, 4\alpha) = \frac{1}{\pi i} \int_0^\pi e^{i\theta - 4\alpha \sin \theta} d\theta$$

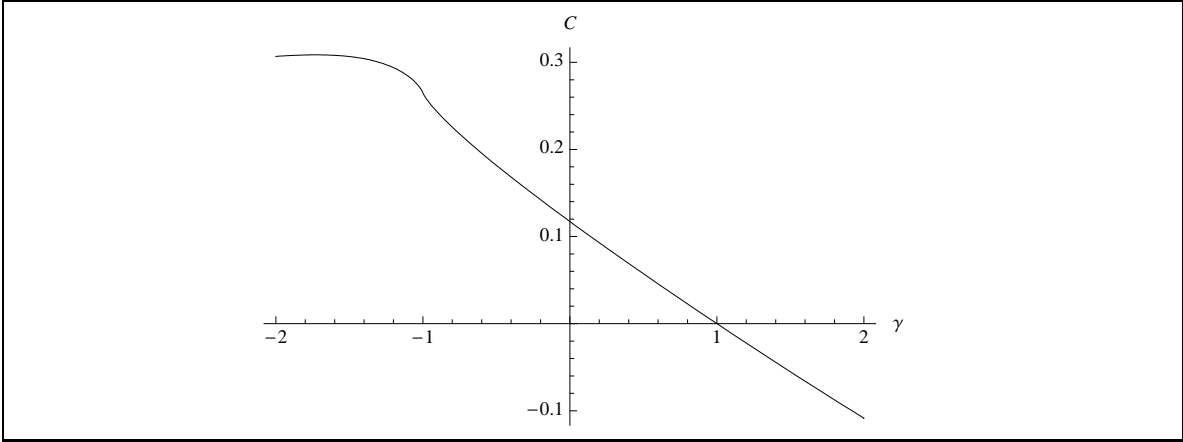


Figure 5: A plot of $C(0.2, \gamma)$, defined in (1.15), for $g \in (-2, 2)$.

where $B_I(n, z)$ is the modified Bessel Function of the first kind of order n and $S_L(n, z)$ is the modified Struve function of order n .

A Pfaffian point process is the analog of a determinantal point process for an anti-symmetric matrix whose entries are given by some integral kernel, with the determinant replaced by a Pfaffian. More information about determinantal processes can be found in [Sos00].

The above theorem gives some information about the covariance between particles located on a horizontal line. From Theorem 4, the covariance between two particles on the same horizontal line is

$$(1.15) \quad C(\alpha, \gamma) := E_1^\gamma(\alpha)^2 - E_2^\gamma(\alpha)^2$$

for $\gamma \neq 1$, where α is the distance between two particles. For $\gamma = 1$, $C(\alpha, 1) = 0$ for all $\alpha \geq 0$. Figure 5 shows a plot of this function for $\alpha = 0.2$. It can be easily shown that $C(\alpha, \gamma)$ is positive if $\gamma < 1$, is negative if $\gamma > 1$ and 0 if $\gamma = 1$.

As in [CCFS89], define the correlation length to be

$$(1.16) \quad \xi(\gamma) := - \lim_{\alpha \rightarrow \infty} \frac{\alpha}{\log(|C(\alpha, \gamma)|)}.$$

This measures the rate of decay of the covariance. In Section 7, we prove the following lemma.

Lemma 2.

$$(1.17) \quad \xi(\gamma) = \begin{cases} \frac{1}{2e_2(\gamma)} & \gamma < -1 \\ \infty & \gamma = -1 \\ \frac{1}{2e_2(\gamma)} & -1 < \gamma < 1 \\ 0 & \gamma = 1 \\ \frac{1}{4} & \gamma > 1 \end{cases}$$

where $e_2(\gamma)$ is defined in Theorem 4.

The discontinuity at $\gamma = 1$ is due to the definition of the correlation length as opposed to any explicit change in phase behavior. This is explained in more detail in Section 7. One further interesting consequence of the above lemma is the following: We have written the model at criticality (i.e. $\gamma = -1$) in terms of the parameter x and taken the scaling window

(x, x^2) . This is an example of the scaling window preserving *scale invariance*. Here, scale invariance means that the correlation length diverges.

For $u = u_\gamma$, the creations (and annihilations) forms a dense set regardless of the value of γ in the scaling window (x, x^2) . This is a consequence of

$$(1.18) \quad \mathbb{E}_\mu[\# \text{ of Creations per fundamental domain}] = \Theta(x^2)$$

for $\mu = \mu(u_\gamma, x)$. In particular, for $\gamma = -1$ (or $u = u_c$), define Γ_ϵ to be the set of creations which give paths of length greater than ϵ in the scaling window (x, x^2) . Provided $\epsilon > 0$, we show that Γ_ϵ is locally finite. In Theorem 6, we show that Γ_ϵ is a Poisson point process with an intensity dependent on ϵ . Unfortunately, our method does not give a specific formula for the intensity.

We have determined the scaling window (x, x^2) of the particle model for $\gamma = 1$. We have also found the distributions of particles along a horizontal line in the scaling window (x, x^2) for all $\gamma \in \mathbb{R}$. We ask the following question, for each u_γ , $\gamma \neq 1$, what is the scaling window (x, x^2) of the particle model? The difficulty lies in the fact that the underlying trajectories of particles are no longer independent, whereas the underlying CNVM construction relies on coalescing but independent random walks (the random walks are independent up to coalescence).

1.7. Overview of the paper. We begin by giving a more rigorous overview of the dimer model on the Fisher lattice, thermodynamic limit and scaling windows. We also provide some calculations concerning Pfaffians that are useful later in the paper. This is all contained in Section 2. In Section 3, we calculate exactly the expected number of **a** and **b** edges covered by dimers in the thermodynamic limit. This leads to finding the expected number of creations or the expected number of annihilations. These provide an insight into the different behavior of the model depending on the value of u . Using the expectations computed in this section, we are able to determine the behavior when $x \rightarrow 0$. We also provide a duality result between high and low anisotropy. In Section 4, we concentrate on the behavior of the model when $u < u_c$ is fixed (and independent of x) and prove Theorem 2. Section 5 provides the proof of Theorem 4 when $\gamma = -1$ and we give the proof of Theorem 6. The case when $u = u_i$ is considered in Section 6, and there, we show the proof that the dimer model when $u = u_i$ is equal in distribution to the noisy voter model. This leads to the convergence to the Continuum Noisy Voter Model. In Section 7, we prove the rest of Theorem 4 (for $\gamma \neq 1, -1$) and also find an explicit expression for the correlation lengths for all values of γ . Section 8 gives some concluding remarks and directions for future work

Acknowledgements: I am very grateful for the help of Richard Kenyon, who provided his valuable insight through countless hours of discussion. I would like to thank David Brydges for many discussions on statistical mechanical models, Jon Warren for pointing out the Brownian Web references, Zhongyang Li for comments on this paper, and Richard Arratia for sending a copy of his PhD thesis, [Arr79].

2. THE DIMER MODEL ON THE FISHER LATTICE

In this section, we introduce some of the theory of the dimer models. Our brief survey contains only the most relevant results crucial for the rest of the paper. For a full treatment of results on dimer models on non-bipartite graphs see [BdT08]. We provide some analysis of the characteristic polynomial (defined in Section 2.2), which sheds some light on the

behavior of the particle model. Finally, we give some facts regarding Pfaffians including an inclusion-exclusion formula.

2.1. Thermodynamic Limit. Let G be a planar graph with structure given by the Fisher lattice, see Figure 1. Suppose that G has edges weights x , ux or 1 depending on whether we have a vertical edge, a non-vertical edge off the triangle decoration or an edge on the triangle decoration. G is \mathbb{Z}^2 -periodic meaning that the action of translations in \mathbb{Z}^2 is an automorphism of G . Let G_n be the quotient of G by the action $n\mathbb{Z}^2$. In other words, G_n is a finite graph, with Fisher lattice structure, on a torus.

A dimer is an edge and a dimer configuration, M , is a subset of edges of G such that each vertex is incident to exactly one edge. For a dimer configuration, we say that a ‘dimer covers an edge’ if that edge is present in the dimer configuration. Let $\mathcal{M}(G)$ denote the set of all dimer configurations of the graph G and let $\mathcal{M}(G_n)$ denote the set of all dimer configurations of the graph G_n . On $\mathcal{M}(G_n)$, define the probability measure μ_n for $M \in \mathcal{M}(G_n)$ by

$$(2.1) \quad \mu_n(M) = \frac{(ux)^{N_b} x^{N_a}}{Z(G_n)}$$

where $N_a = N_a(M)$ and $N_b(M)$ are the numbers of dimers covering **a** and **b** edges in the dimer configuration M and $Z(G_n)$ is the partition function: $Z(G_n) = \sum_{M \in \mathcal{M}(G_n)} (ux)^{N_b} x^{N_a}$. A measure of the form in (2.1) is called a Boltzmann measure.

A Gibbs measure on $\mathcal{M}(G)$ has the following property: Fixing the perfect matchings inside an annular region, then the perfect matchings inside and outside of this annular region are independent. Let \mathcal{F} be the σ -field generated by cylinders (here, a cylinder is the set of dimer configurations of G containing a fixed finite subset of edges of G). Then, Theorem 6 of [BdT08] guarantees the existence of a unique probability Gibbs measure $\mu = \mu(u, x)$ defined on $(\mathcal{M}(G), \mathcal{F})$ such that it is weak limit of the Boltzmann measures μ_n as $n \rightarrow \infty$ for any dimer model on a non-bipartite graph. This limiting measure is called the *thermodynamic limit*. We denote $\mu_0 = \lim_{x \rightarrow 0} \mu(u, x)$, $\mathbb{P}_\mu(\cdot)$ to be the probability of the event (\cdot) under μ and \mathbb{E}_μ to be the expectation under μ .

2.2. Partition Function, Local Probabilities and Notation. Here, we explain some of the theory of dimer models. In particular, we state results that are useful in the rest of the paper, such as, the formula for the partition function and local statistics formula. For proofs of these results, see [BdT08].

We refer to the graph G_1 as the fundamental domain. Orient the edges of G_1 so that the number of counter clockwise edges per face is odd. This is called the *Kastelyn orientation*. Such an orientation is given in Figure 6 for the fundamental domain. Assume that G (the infinite planar graph) has the periodic Kastelyn orientation induced by G_1 . As G is \mathbb{Z}^2 periodic, we can write any vertex of G as a vertex of G_1 plus a translation of the fundamental domain, where the first co-ordinate of the translation is in the direction of the vector $(1, 1)$ and the second co-ordinate is in the direction of the vector $(-1, 1)$ (i.e. $v + (x, y)$ is the vertex v in the fundamental domain translated by $(x - y, x + y)$).

Let $V(G_1) = \{v_i\}$ be the set of vertices of G_1 labelled as per Figure 6. Let γ_1 (and resp. γ_2) be a path in the dual of G_1 , winding around the torus in the direction of the vector $(1, 1)$ (and $(-1, 1)$). Write e_{ij} for the weight of the edge $\overrightarrow{v_i v_j}$. For parameters z and w , let

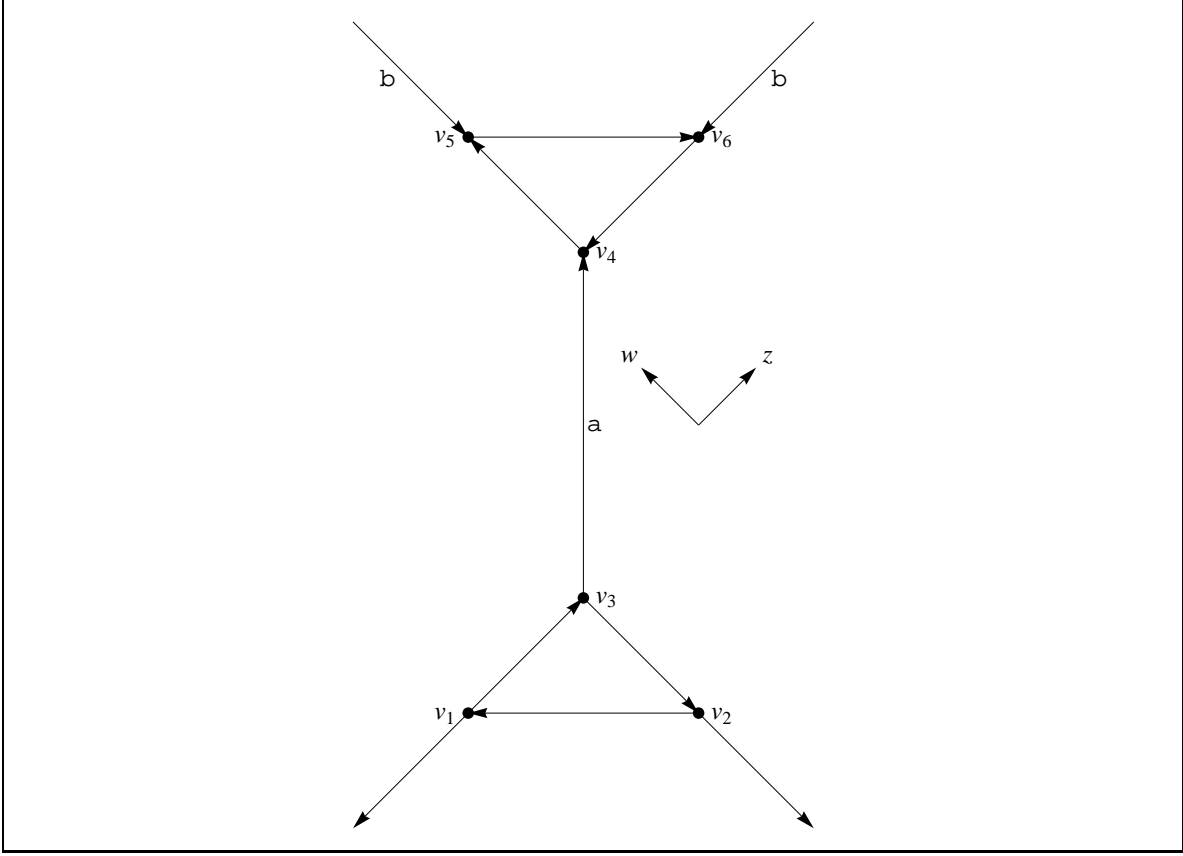


Figure 6: Fundamental domain. The edge from v_1 to v_6 crosses γ_1 and the edge from v_2 to v_5 crosses γ_2 .

$w_{ij} = z^{n_1} w^{n_2} e_{ij}$, where

$$(2.2) \quad n_1(n_2) = \begin{pmatrix} 1 & \overrightarrow{v_i v_j} \text{ crosses } \gamma_1(\gamma_2) \text{ from below} \\ 0 & \overrightarrow{v_i v_j} \text{ does not cross } \gamma_1(\gamma_2) \\ -1 & \overrightarrow{v_i v_j} \text{ crosses } \gamma_1(\gamma_2) \text{ from above} \end{pmatrix}$$

Let $K(z, w)$ be the 6×6 anti-symmetric matrix given by

$$(2.3) \quad (K(z, w))_{i,j} = \begin{cases} w_{ij} & \text{if } v_i \sim v_j, \text{ and } v_i \rightarrow v_j \\ -w_{ij} & \text{if } v_i \sim v_j, \text{ and } v_j \rightarrow v_i \\ 0 & \text{otherwise} \end{cases}$$

where $v_i \sim v_j$ means that v_i and v_j share an edge and $v_i \rightarrow v_j$ denotes an arrow from v_i to v_j in the Kastelyn orientation. This gives

$$(2.4) \quad K(z, w) = \begin{pmatrix} 0 & -1 & 1 & 0 & 0 & b/z \\ 1 & 0 & -1 & 0 & b/w & 0 \\ -1 & 1 & 0 & a & 0 & 0 \\ 0 & 0 & -a & 0 & 1 & -1 \\ 0 & -bw & 0 & -1 & 0 & 1 \\ -bz & 0 & 0 & 1 & -1 & 0 \end{pmatrix}.$$

where $a = x$ and $b = ux$.

The relevance of the above discussion is that we can write the partition function and probabilities of observing a local configuration in the thermodynamic limit as expressions involving $K(z, w)$ (see [BdT08] and [KOS06]). The characteristic polynomial for the fundamental domain, $P(z, w)$, is defined to be the determinant of $K(z, w)$. This gives

$$(2.5) \quad P(z, w) = a^2 + 2b^2 + a^2b^4 + ab(1 - b^2)\left(z + \frac{1}{z} + w + \frac{1}{w}\right) + b^2(1 - a^2)\left(\frac{z}{w} + \frac{w}{z}\right)$$

The logarithm of the partition function can be written in terms of the characteristic polynomial, namely

$$(2.6) \quad \log Z = -\frac{1}{2(4\pi^2)} \int_{|z|=1} \int_{|w|=1} \log P(z, w) \frac{dw}{w} \frac{dz}{z}$$

Let $E = \{e_1 = u_1u_2, \dots, e_m = u_{2m-1}u_{2m}\}$ be a subset of edges, with each u_i representing a distinct vertex. [BdT08] showed that the probability of observing E in thermodynamic limit is given by

$$(2.7) \quad \mathbb{P}_\mu(e_1, \dots, e_m) = \left(\prod_{i=1}^m K(u_{2i}, u_{2i+1}) \right) \text{Pf} \left((K^{-1}(u_i, u_j))^T \right)_{1 \leq i, j \leq 2m}$$

where T represents the transpose of a matrix and assuming v and \tilde{v} are in the same fundamental domain,

$$(2.8) \quad K^{-1}(v, \tilde{v} + (x, y)) = \frac{1}{(2\pi i)^2} \int_{\mathbb{T}^2} K^{-1}(z, w)_{v, \tilde{v}} w^x z^y \frac{dw}{w} \frac{dz}{z}.$$

This formula was discovered in [Ken97] for bipartite graphs. (2.7) is referred to as the *local statistics formula*.

For the rest of the paper, we use the following notation. We denote $v_i(n, m) = v_i + (n, m)$ where $i \in \{1, 6\}$. In other words, $v_i(n, m)$ is the vertex v_i in the (n, m) fundamental domain. Note that $v_i = v_i(0, 0) = v_i + (0, 0)$.

2.3. Critical Values. In this subsection, we allow $u \in (0, \infty)$. A dimer model is said to be *critical* if there exists values of $(z, w) \in \mathbb{T}^2$ such that $P(z, w) = 0$. The dimer model on the Fisher lattice with weights (u, x) is critical when $(-1 + \sqrt{1 + x^2})/x^2$ and $(1 + \sqrt{1 + x^2})/x^2$. By Lemma 7, the particle model has the same distribution at each of these values of u . We define u_c to be $(-1 + \sqrt{1 + x^2})/x^2$, which is approximately $1/2 - x^2/8$. The dimer model on the Fisher lattice has other values of interest, namely $(1 - \sqrt{1 - x^2})/x^2$ and $(1 + \sqrt{1 - x^2})/x^2$. Again, the particle model has the same distribution at each of these values of u by Lemma 7. We define u_i to be $(1 - \sqrt{1 - x^2})/x^2$ and refer to it as the *independent value* of u . The details of $u = u_i$ and why it forms an ‘independent’ model is contained in Section 6.

2.4. Particle Model probability space. In this subsection, we define the underlying probability space for the particle model by use of a certain metric. We use the same space defined in [AB99] and [Cam08]. Let \mathbb{R}^2 denote $\mathbb{R}^2 \cup \{\infty\}$, i.e. the compactification of \mathbb{R}^2 . Let d be the spherical metric, which is defined to be $d : \mathbb{R}^2 \times \mathbb{R}^2 \rightarrow \mathbb{R}$ by

$$(2.9) \quad d(u, v) = \inf \int (1 + |\phi|^2)^{-1} ds$$

where the infimum is over all smooth curves connecting u and v , ϕ is parameterized by the arc length s and $|\cdot|$ is the Euclidean metric.

Let \mathcal{H} be the space of all collections of curves in \mathbb{R}^2 . We need to define a metric on \mathcal{H} in order to determine its open sets. Let γ_1 and γ_2 be two curves with their parametrization at

time t given by $\gamma_1(t)$ and $\gamma_2(t)$. Consider a complete separable metric space S of continuous curves in \mathbb{R}^2 , with distance given by

$$(2.10) \quad D(\gamma_1, \gamma_2) = \inf \sup_{t \in [0,1]} d(\gamma_1(t), \gamma_2(t))$$

where the infimum is over all choices of parametrizations of γ_1 and γ_2 . The collection of all closed sets of S is exactly \mathcal{H} . Let \mathcal{F}_1 and \mathcal{F}_2 denote two closed sets of curves. Then, D induces the Hausdorff metric, $D_{\mathcal{H}}$, defined by

$$(2.11) \quad D_{\mathcal{H}}(\mathcal{F}_1, \mathcal{F}_2) < \epsilon \Rightarrow (\forall \gamma_1 \in \mathcal{F}_1, \exists \gamma_2 \in \mathcal{F}_2 \text{ such that } D(\gamma_1, \gamma_2) < \epsilon \text{ and vice versa})$$

Therefore, $(\mathcal{H}, D_{\mathcal{H}})$ defines a complete separable metric space. Let $\mathcal{F}_{\mathcal{H}}$ denote the Borel σ field associated with the metric $D_{\mathcal{H}}$. Let $\mathcal{M}_{\mathcal{H}}$ be the space of probability measures taking values in $(\mathcal{H}, \mathcal{F}_{\mathcal{H}})$. It is clear that the particle model (before rescaling) are measures in the space $\mathcal{M}_{\mathcal{H}}$ for all values of u and x .

We remind the reader that we say the scaling window (x^α, x^β) of some measure is the limiting measure obtained when taking the box (x^α, x^β) to $(1, 1)$ while simultaneously sending $x \rightarrow 0$. It is evident that the CNVM is in $\mathcal{M}_{\mathcal{H}}$ because the Brownian Web (through which the CNVM is constructed) is a random variable taking values in $(\mathcal{H}, \mathcal{F}_{\mathcal{H}})$. For each u_γ and $\gamma \neq 1$, it is expected that the limiting measure of the particle model in the scaling window (x, x^2) is in $\mathcal{M}_{\mathcal{H}}$.

For $u < u_c$ (u is independent of x), it is enough to consider the space $\mathcal{M}_{\mathbb{R}^2}$, which is the space of locally finite point processes on \mathbb{R}^2 , for the particle model. This is due to showing, in Section 4, that there are no infinite lines and the loops formed by the trajectories of pairs of particles are finite \mathbb{P}_μ -almost surely.

For each u_γ and $\gamma \neq 1$, the distribution of the locations of particles along an arbitrary horizontal line is contained in $\mathcal{M}_{\mathbb{R}}$, the space of locally finite point process on \mathbb{R} . By choosing the scaling window so that the density of particles along a horizontal line remains constant, the distribution of particles along this horizontal line converges to some measure in $\mathcal{M}_{\mathbb{R}}$. This limiting measure, under the appropriate re-scaling, is found in Theorem 4.

2.5. Distribution of many particles. This self-contained subsection focuses on a formula for the locations of particles in the particle model. Essentially, this formula is an inclusion-exclusion type formula. We prove it using the recursive definition of the Pfaffian. However, another proof of the formula can be found using the fact that a Pfaffian of an anti-symmetric matrix can be thought of counting perfect matchings of a weighted graph (negative weights are allowed here), see [God93] for more details.

The notation is set up to avoid explicitly writing out complete matrices. For $1 \leq i \leq n$, let X_i represent the existence of a particle at x_i . This is equivalent to the appropriate **a** edge not being covered by a dimer in the underlying dimer configuration. The complement of X_i shall be denoted X_i^c , which represents a dimer covering the appropriate **a** edge in the underlying dimer configuration. Let \mathbb{P} denote the law of observing the particles. Let $K_n(x_1, \dots, x_n) = \{k_{i,j}\}_{i,j=1}^{2n}$ represent the $2n$ by $2n$ anti-symmetric matrix with $k_{2i-1,2i} = v = \mathbb{P}(X_i^c)$ for $1 \leq i \leq n$ and $k_{i,j}$ denote the appropriate inverse Kastelyn entries so that

$$(2.12) \quad \mathbb{P}(X_1^c, \dots, X_n^c) = \text{Pf}(K_n(x_1, \dots, x_n))$$

Define, $K_n(\hat{x}_1, \dots, \hat{x}_k, x_{k+1}, \dots, x_n) = \{\hat{k}_{i,j}\}_{i,j=1}^{2n}$, with $\hat{k}_{2i-1,2i} = -1 + v$ for $1 \leq i \leq k$ and $\hat{k}_{i,j} = k_{i,j}$. Let $I_n^{sk} = \{a_{i,j}\}_{i,j=1}^{2n}$ represent the antisymmetric matrix with $a_{2i-1,2i} = 1$ for $i \in \{1, \dots, n\}$ and $a_{i,j} = 0$ otherwise. Then

Lemma 3.

$$(2.13) \quad \mathbb{P}(X_1, \dots, X_n) = \text{Pf}(I_n^{sk} - K_n(x_1, \dots, x_n)) = (-1)^n \text{Pf}(K_n(\hat{x}_1, \dots, \hat{x}_n))$$

The proof does not require the edges covered to have the same probability of being covered. The result is stated in this fashion for convenience later in the paper.

Proof. The proof follows by using an iteration, with the key step relying on using the recursive definition of the Pfaffian. Consider

$$(2.14) \quad \mathbb{P}(X_1, X_2^c, \dots, X_n^c) = \mathbb{P}(X_2^c, \dots, X_n^c) - \mathbb{P}(X_1^c, \dots, X_n^c)$$

with $\mathbb{P}(X_2^c, \dots, X_n^c) = \text{Pf}(K_{n-1}(x_2, \dots, x_n))$ and $\mathbb{P}(X_1^c, \dots, X_n^c)$ is given in (2.12). On the other hand, by using the recursive definition of the Pfaffian and letting $A = K_n(\hat{x}_1, x_2, \dots, x_n)$

$$(2.15) \quad \text{Pf}(K_n(\hat{x}_1, x_2, \dots, x_n)) = (-1 + v) \text{Pf}(A_{\hat{1}, \hat{2}}) + \sum_{i=3}^{2n} (-1)^i k_{1,i} \text{Pf}(A_{\hat{1}, \hat{i}})$$

where $A_{\hat{1}, \hat{i}}$ is the matrix obtained by removing both the 1st and i^{th} row and column. Notice that $\text{Pf}(A_{\hat{1}, \hat{2}})$ is exactly $\text{Pf}(K_{n-1}(x_2, \dots, x_n))$ while $v \text{Pf}(A_{\hat{1}, \hat{2}}) + \sum_{i=3}^{2n} (-1)^i k_{1,i} \text{Pf}(A_{\hat{1}, \hat{i}}) = \text{Pf}(K_n(x_1, x_2, \dots, x_n))$. Therefore, substituting (2.15) into (2.14) gives

$$(2.16) \quad \mathbb{P}(X_1, X_2^c, \dots, X_n^c) = -\text{Pf}(K_n(\hat{x}_1, x_2, \dots, x_n)).$$

Applying the steps to obtain (2.16) iteratively gives the result. \square

3. THERMODYNAMIC LIMIT

This section focuses on the behavior of the model in the thermodynamic limit. We introduce a generic method for calculating expectations, which is shown by computing the expected number of dimers covering **b** edges per fundamental domain. This method can be used to compute other expectations, such as the expected number of dimers covering **a** edges per fundamental domain. We then use expansions of the computed expectations to find the behavior of the model in the limit $x \rightarrow 0$. All the results are reliant on analysis of $P(z, w)$, which we provide later in the section. Finally, we state and prove a ‘duality’ statement for low and high anisotropy.

3.1. Expectations for $0 < x < 1$ and $0 < u < 1$. Let N_b denote the number of dimers covering **b** edges per fundamental domain. By the setup of the model, there are 2 **b** edges in each fundamental domain. Let N_{ac} denote the number of **a** edges not covered by a dimer per fundamental domain. Let N_X denote the number of creation singularities per fundamental domain. In this subsection, we find exact results for $\mathbb{E}_\mu[N_b]$, $\mathbb{E}_\mu[N_{ac}]$ and $\mathbb{E}_\mu[N_X]$. Figure 7 shows a plot of $\mathbb{E}[N_b]$ and $\mathbb{E}[N_a]$ for $x = 0.5$. Recall that we defined $u_c = (-1 + \sqrt{1 + x^2})/x^2$.

Theorem 5. For $0 < x < 1$ and $0 < u < 1$

$$(3.1) \quad \mathbb{E}_\mu[N_b] = \begin{cases} f(x, u, r) + \frac{2u^2 x^2}{-1 + u^2 x^2} & \text{if } u < u_c \\ f(x, u, 1) + \frac{2u^2 x^2}{-1 + u^2 x^2} & \text{if } u = u_c \\ f(x, u, 1/r) + \frac{2u^2 x^2}{-1 + u^2 x^2} & \text{if } u > u_c \end{cases}$$

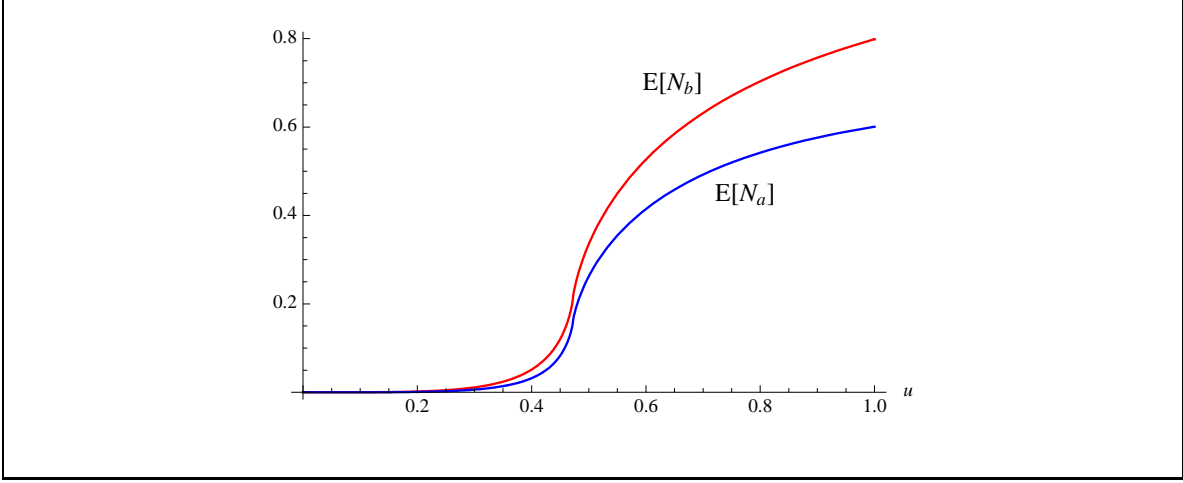


Figure 7: A plot of $\mathbb{E}[N_b]$ and $\mathbb{E}[N_a]$ against $u \in (0, 1)$ for $x = 0.5$. Notice that the difference between the two curves is $2\mathbb{E}[N_X]$.

where $f(x, u, r)$ is a continuous function given by

(3.2)

$$f(x, u, r) = C(x, u)((u^2(-1 + x^2) + r^2u^2(-1 + x^2) + r(1 + u^4x^4 - 2u^2(1 + 2x^2)))\mathcal{K}\left(\frac{r-s}{rs-1}\right) + C(x, u)(-1 + r^2)u^2(-1 + x^2)\left(\Pi\left(\frac{r(r-s)}{rs-1}, \frac{r-s}{rs-1}\right) - \Pi\left(\frac{r-s}{rs-1}, \frac{r-s}{rs-1}\right)\right)$$

for $r \neq 1$ where

$$(3.4) \quad C(x, u) = \frac{\sqrt{rs}(1 + u^2x^2)}{\pi r(rs - 1)u^2(-1 + x)(1 + x)(-1 + u^2x^2)},$$

$$(3.5) \quad r = \frac{-1 + 2u^2 - u^4x^4 + (-1 + u^2x^2)\sqrt{1 - 4u^2 + 2u^2x^2 + u^4x^4}}{2(-u - 2u^2x - u^2x^2)},$$

$$(3.6) \quad s = \frac{1 - 2u^2 - u^4x^4 + (-1 + u^2x^2)\sqrt{1 - 4u^2 + 2u^2x^2 + u^4x^4}}{2(-u + 2u^2x - u^2x^2)}.$$

$\mathcal{K}(k)$ represents the complete elliptic integral of the first kind with modulus k and $\Pi(n, k)$ represents the complete elliptic of the third kind with characteristic n and modulus k . Also,

$$(3.7) \quad f(x, u, 1) = \frac{(-1 - x^2 + \sqrt{1 + x^2})(-2 - x^2 + 2\sqrt{1 + x^2})}{(-1 + \sqrt{1 + x^2})^3} \left(-\frac{1}{2\pi i} \log \frac{x+i}{x-i} + 1 \right)$$

The elliptic integrals are defined for $u > u_c$ by an analytic continuation argument (see [Law89]). Note that $\mathbb{E}_\mu[N_b]$ is a continuous function.

Proof. There are two ways to compute $\mathbb{E}_\mu[N_b]$. Either use the inverse Kasteleyn matrix to compute the probability of seeing an edge along v_5 to v_2 (and multiply the corresponding result by 2) or we can use the properties of the partition function. We follow the latter approach. Differentiating under the integral sign in (2.6) with respect to b and multiplying

by b gives

$$(3.8) \quad \mathbb{E}_\mu[N_b] = \frac{b}{8\pi^2} \int_{|w|=1} \int_{|z|=1} \frac{\frac{\partial}{\partial b} P(z, w)}{P(z, w)} \frac{dz}{z} \frac{dw}{w}$$

Taking the change of variable $z = vw$ gives

$$(3.9) \quad \mathbb{E}_\mu[N_b] = \frac{b}{8\pi^2} \int_{|w|=1} \int_{|z|=1} \frac{\frac{\partial}{\partial b} P(vw, w)}{P(vw, w)} \frac{dv}{v} \frac{dw}{w}$$

Setting $a = x$, $b = ux$, then the roots of the denominator of the integrand with respect to w are given by 0, $r_1(v)$ and $r_2(v)$, where

$$(3.10) \quad \frac{1}{2(uv + uv^2 - u^3vx^2 - u^3v^2x^2)} (-u^2 - v - 2u^2v - u^2v^2 + u^2x^2 + u^2v^2x^2 - u^4vx^4 \mp A(v))$$

where

$$(3.11) \quad A^2(v) = (-4(u + uv - u^3x^2 - u^3vx^2)(uv + uv^2 - u^3vx^2 - u^3v^2x^2) + (u^2 + v + 2u^2v + u^2v^2 - u^2x^2 - u^2v^2x^2 + u^4vx^4)^2).$$

The root $r_1(v)$, lies within the region $|w| < 1$ for all $|v| < 1$ while $r_2(v)$, lies in the region $|w| > 1$ for all $|v| < 1$. Therefore, the first integral in (3.9) can be evaluated using residue calculus.

The residue at $w = 0$ for (3.9) is given by

$$(3.12) \quad \frac{ux}{2} \frac{1}{2\pi i} \int_{|v|=1} \frac{-1 + 3u^2x^2}{uvx(-1 + u^2x^2)} dv = \frac{1 - 3u^2x^2}{2(1 - u^2x^2)}$$

The residue at $w = r_1(v)$ for (3.9) is more complicated and is given by

$$(3.13) \quad \frac{1}{2\pi i} \int_{|v|=1} \frac{Q(v)}{2v(-1 + u^2x^2)A(v)} dv.$$

where

$$(3.14) \quad Q(v) = (1 + u^2x^2)(v + u^4vx^4 + u^2(-1 + x^2 + v^2(-1 + x^2) - 2v(1 + 2x^2)))$$

The residue at $v = 0$ for (3.13) is given by

$$(3.15) \quad \frac{1 + u^2x^2}{-2(1 + u^2x^2)}.$$

Notice that the contribution from (3.12) and (3.15) is $\Theta(x^2)$ and gives the additive term shown in the formula for $\mathbb{E}_\mu[N_b]$. It remains to finish evaluating (3.13), which is done by analysis of the roots of $A(v)$. The roots of $A(v)$ are $r, s, 1/r, 1/s$, where r and s are defined in Theorem 5. The behavior of the underlying dimer model is dependent on the location of these four roots, which is given explicitly in Section 3.3.

Notice that $|s| > 1$ for all values of u . However, $|r| > 1$ if $u < u_c$, $r = 1$ if $u = u_c$ and $|r| < 1$ if $u > u_c$. We can consider each case separately. Note that when $u = u_i > u_c$, $A(v)$ breaks down into a quadratic. In this special case, we can calculate using residue calculations.

For $u < u_c$, the contour of integration in (3.13) can be deformed to a contour integral surrounding the branch cut from $1/r$ to $1/s$ as the residue at $v = 0$ has already been considered. This integral can then be deformed further giving two line integrals, which can

both be written as integrals from $1/r$ to $1/s$. These integrals are given by elliptic integrals, which can be simplified to the desired form.

For $u = u_c$, then $A(v)$ is given by

$$(3.16) \quad (v-1)\sqrt{(v-s)(v-1/s)}.$$

This implies that the contour of integration in (3.13) can be deformed to a contour integral surrounding 1 and $1/s$. Completing the integrals via line integrals gives the required result.

For $u > u_c$, then we can repeat the same steps as given for $u < u_c$ but with the branch cut running from r and $1/s$. □

Corollary 1. For $0 < x < 1$ and $0 < u < 1$,

$$(3.17) \quad \mathbb{E}_\mu[N_{a^c}] = \begin{cases} g(x, u, r) - \frac{x^2}{1-x^2} & \text{if } u < u_c \\ g(x, u, 1) - \frac{x^2}{1-x^2} & \text{if } u = u_c \\ g(x, u, 1/r) - \frac{x^2}{1-x^2} & \text{if } u > u_c \end{cases}$$

where

$$(3.18) \quad \begin{aligned} g(x, u, r) = & D(x, u)(u^2(1+x^2) + r^2u^2(1+x^2) - r(1-2u^2+u^4x^4))K\left(\frac{(r-s)}{(-1+rs)}\right) \\ & + D(x, u)(-1+r^2)u^2(1+x^2)\left(\Pi\left(\frac{r(r-s)}{rs-1}, \frac{r-s}{rs-1}\right) - \Pi\left(\frac{r-s}{rs-1}, \frac{r-s}{rs-1}\right)\right) \end{aligned} \quad (3.19)$$

for $r \neq 1$, where $D(x, u) = C(x, u)(-1+u^2x^2)/(1+u^2x^2)$, $C(x, u)$, r , s , K and Π are defined in Theorem 5. Finally,

$$(3.20) \quad g(x, u, 1) = \frac{1+x^2}{1-x^2} \left(1 - \frac{1}{\pi i} \log\left(\frac{x+i}{x-i}\right)\right)$$

Proof. $\mathbb{E}_\mu[N_{a^c}]$ can either be computed using the partition function or by using inverse Kastelyn techniques, namely

$$(3.21) \quad \mathbb{E}_\mu[N_{a^c}] = 1 - xK^{-1}(v_3, v_4).$$

This can be computed using the same techniques used in Theorem 5. □

A creation consists of 3 edges, so its expectation consists of a Pfaffian of a 12 by 12 matrix. This is somewhat messy. However, the next lemma shows that $\mathbb{E}_\mu[N_X]$ can be computed using $\mathbb{E}_\mu[N_b]$ and $\mathbb{E}_\mu[N_{a^c}]$.

Lemma 4.

$$(3.22) \quad \mathbb{E}_\mu[N_X] = \frac{1}{2} (\mathbb{E}_\mu[N_b] - \mathbb{E}_\mu[N_{a^c}])$$

Proof. The trajectories of paths in the particle model form loops and infinite lines. These can be represented on the underlying dimer model as dimers covering **b** edges and not covering **a** edges. Let \hat{N}_b denote the number of dimers covering **b** edges, which do not belong to creations, per fundamental domain. Clearly, for each loop or line, $\hat{N}_b = N_{a^c}$ and

$$(3.23) \quad \mathbb{E}_\mu[\hat{N}_b] = \mathbb{E}_\mu[N_{a^c}].$$

On the other hand, $2N_X = N_b - \hat{N}_b$ because for each loop or infinite line, the difference $N_b - \hat{N}_b$ is the number of pairs of \mathbf{b} edges seen in a fundamental domain (per fundamental domain). These are exactly creations (from definition of \hat{N}_b). Therefore,

$$(3.24) \quad \mathbb{E}_\mu[N_b] - \mathbb{E}_\mu[\hat{N}_b] = 2\mathbb{E}_\mu[N_X]$$

Combining (3.23) and (3.24) gives the result. \square

This leads to the following

Corollary 2. *For $0 < x < 1$ and $0 < u < 1$*

$$(3.25) \quad \mathbb{E}_\mu[N_X] = \begin{cases} \frac{1}{2} \left(f(x, u, r) - g(x, u, r) - \frac{x^2(1-2u^2+u^2x^2)}{(1-x^2)(1-u^2x^2)} \right) & \text{if } u < u_c \\ \frac{1}{2} \left(f(x, u, 1) - g(x, u, 1) - \frac{x^2(1-2u^2+u^2x^2)}{(1-x^2)(1-u^2x^2)} \right) & \text{if } u = u_c \\ \frac{1}{2} \left(f(x, u, r) - g(x, u, r) - \frac{x^2(1-2u^2+u^2x^2)}{(1-x^2)(1-u^2x^2)} \right) & \text{if } u > u_c \end{cases}$$

where the functions f and g are defined in Theorem 3.9 and Corollary 1.

3.2. Expectations in the limit $x \rightarrow 0$. The results in the previous subsection can be expanded out in terms of x for some values of u . By computing the expansions of $\mathbb{E}_\mu[N_b]$ and $\mathbb{E}_\mu[N_X]$, we can determine the behavior of the model in the limit $x \rightarrow 0$. This does require some attention - taking the limit through the underlying integrals cannot always be done. Therefore, we need careful expansion of the appropriate elliptic integrals.

Lemma 5.

$$(3.26) \quad \mathbb{E}_\mu[N_b] = \begin{cases} O(x^2) & \text{if } u < u_c \text{ (fixed)} \\ \frac{2x}{\pi} + O(x^2) & \text{if } u = u_c \\ x + O(x^2) & \text{if } u = u_i \\ 2 - 2\frac{\theta}{\pi} + O(x) & \text{if } u > u_i \text{ (fixed)} \end{cases}$$

where $\theta = \arccos(-1/(2u))$. Furthermore, the first order term of $\mathbb{E}_\mu[N_{a^c}]$ is equal to the first order term of $\mathbb{E}_\mu[N_b]$ in each case.

Note that $2/\pi < E[N_{a^c}] < x$ and $\mathbb{E}_\mu[N_{a^c}]$ is increasing for $u_c < u < u_i$ by (7.5). The same is true for $\mathbb{E}_\mu[N_b]$.

Proof. For $u < u_c$ (fixed), the modulus of the elliptic integrals, $k = (s - r)/(rs - 1) = 4u^2x/\sqrt{1 - 4u^2} + O(x)$. The expansions of the elliptic integrals are given by

$$(3.27) \quad \mathcal{K}(k) = \frac{\pi}{2} + \frac{k^2\pi}{4} + O(k^4)$$

and

$$(3.28) \quad \Pi(rk, k) - \Pi(k/r, k) = \frac{k\pi(-1 + r^2)}{4r} + \frac{3k^2\pi(-1 + r^4)}{16r^2} + O(k^3).$$

Expanding r and s in terms of x and simplifying gives the result.

The expansion for $u = u_c$ follows by a series expansion of the expression given in Theorem 5.

For $u = u_i$, we can calculate $\mathbb{E}_\mu[N_b]$ using solely residue calculations. This is due to the branch cuts contract to a point. Hence, $A(v)$ defined in the proof of Theorem 5 is a quadratic.

For $u > u_i$ (fixed), the modulus of each of the elliptic integrals is given by i/k' where $k' = |s/r - 1|/|s - 1/r| = 4u^2x/\sqrt{4u^2 - 1} + O(x)$ and $i = \sqrt{-1}$. The expansions for the elliptic integrals are given by

$$(3.29) \quad \mathcal{K}(k) = k' \log \left(\frac{2}{k'} \right) + k' \log 2 + O(k'^2)$$

and

$$(3.30) \quad \Pi \left(\frac{ir}{k}, \frac{i}{k'} \right) - \Pi \left(\frac{i}{rk'}, \frac{i}{k'} \right) = k' \log \frac{1}{r} + O(k'^2).$$

which are both computed in the Appendix of [Chh11]. Plugging back the relevant expressions gives the result.

The last statement follows by finding the expansions $\mathbb{E}_\mu[N_{ac}]$ which is achieved using the same method. \square

The expansion for $\mathbb{E}_\mu[N_X]$ can be also computed for certain values of u . This is given by the following

Lemma 6.

$$(3.31) \quad \mathbb{E}_\mu[N_X] = \begin{cases} \frac{1}{2}(1 - 2u^2 - \sqrt{1 - 4u^2})x^2 + O(x^3) & \text{if } u < u_c \text{ (fixed)} \\ \frac{x^2}{4} + O(x^3) & \text{if } u = u_c \\ \frac{x^2}{4} + O(x^3) & \text{if } u = u_i \\ (-\frac{1}{\pi}\sqrt{4u^2 - 1})x^2 \log x + O(x^2) & \text{if } u > u_i \text{ (fixed)} \end{cases}$$

Proof. For $u = u_i$ or $u = u_c$, the exact same method employed in the proof of Lemma 5 holds. Otherwise, notice that $\mathbb{E}_\mu[N_X]$ is of the form

$$(3.32) \quad c_1(x, u)K(k) + c_2(x, u)(\Pi(r/k, k) - \Pi(1/(rk), k) + O(x^2))$$

where $c_1(x, u), c_2(x, u)$ represent coefficients of the complete elliptic integrals and k represents the appropriate modulus of the elliptic integrals, given in Theorem 5. For $u < u_c$, c_1 and c_2 are both of $O(x^2)$, hence the expansions of the elliptic integrals given in the proof of Lemma 5 hold for $u < u_c$. When $u > u_i$, $c_1(x, u)$ are both $O(x)$, which implies that we can use the expansions for the elliptic integrals in their given form, without needing to compute extra terms. \square

We can now prove Theorem 1.

Proof of Theorem 1. For $u \in (0, 1)$, using Markov's inequality and the Borel-Cantelli Lemmas, we obtain

$$(3.33) \quad \lim_{x \rightarrow 0} \mathbb{P}_\mu(N_X = 0) = 1.$$

As the distribution of the creations is the same as the distribution of the annihilations, (3.33) implies with probability 1, there are no annihilations or creations for $u \in (0, 1)$. By Lemma 5, in the limit $x \rightarrow 0$ and $u > 1/2$, particles have density $2 - 2\theta/\pi$. For $u \leq 1/2$, by applying Markov's inequality and the Borel-Cantelli Lemmas,

$$(3.34) \quad \lim_{x \rightarrow 0} \mathbb{P}_\mu(N_{ac} = 0) = 1$$

\square

3.3. Analysis of $P(z, w)$. This subsection is primarily a consequence of the calculation in Theorem 5. We provide the behavior of the roots of $A(v)$, defined in (3.11). As a consequence, we can prove a ‘duality’ result, which gives an isometry for high and low anisotropy.

Recall that $P(z, w) = \det K(z, w)$ represents the characteristic polynomial and that a dimer model is said to be *critical* if $P(z, w) = 0$ for some $(z, w) \in \mathbb{T}^2$. Recall that $r, s, 1/r, 1/s$ are the roots of $A(v)$, as defined in (3.11). The values of the roots of $A(v)$ are dependent on the anisotropy as follows:

- For $u < u_c$, the roots are $r, s, 1/r$ and $1/s$ for $r, s \in \mathbb{R}$ with $1 < r < s$.
- For $u = u_c$, the roots are $s, 1$ (twice) and $1/s$ for $s \in \mathbb{R}$ with $1 < s$.
- For $u_c < u < u_i$, the roots are $r, s, 1/r$ and $1/s$ for $r, s \in \mathbb{R}$ with $r < 1 < s$.
- For $u = u_i$, the roots are r (twice) and $1/r$ (twice) for $r \in \mathbb{R}$ with $r < 1$.
- For $u > u_i$ ($u < 1/x$), the roots are $r, \bar{r}, 1/r$ and $1/\bar{r}$ for $r \in \mathbb{C}$ with $|r| < 1$.

It is evident that for $u = u_c$, $A(-1) = 0$, which implies the model is critical when $u = u_c$. Taking $u = u_i$, then all entries in the inverse Kastelyn matrix can be computed solely using residue calculations. This leads to the model possessing independent trajectories of particles (see Section 6 for further details).

Provided that $u \in (0, 1)$, at low temperature the distance between certain pairs of roots is $O(x)$. For $u \leq u_i$, $r - s$ is $O(x)$. For $u > u_i$, $r - 1/\bar{r}$ is $O(x)$. Notice that choosing $u = 1/2 + x^a c$ for $0 < a \leq 2$ and c is a constant, $r - 1/r$ is $O(x^{a/2})$.

The next lemma gives a ‘duality’ for ux . Here, we temporarily drop the assumption that $u \in (0, 1)$. Let X denote any configuration of \mathbf{a} edges not covered by dimers in the dimer configuration. For notational simplicity, write $\mathbb{P}_{\mu(u, x)} = \mathbb{P}(u, x, X)$.

Lemma 7. *For $u < 1/x$ and $x > 0$,*

$$(3.35) \quad \mathbb{P}(u, x, X) = \mathbb{P}\left(\frac{1}{ux^2}, x, X\right)$$

This shows that the particle model has the same distribution when choosing the anisotropy to be either $1/(ux^2)$ or u , provided $u < 1/x$. This also implies that the two critical points $(-1 + \sqrt{1+x^2})/x^2$ and $(1 + \sqrt{1+x^2})/x^2$ are equivalent (in distribution) in terms of the particle model as $(1 + \sqrt{1+x^2})/x^2 = 1/(u_c x^2)$.

Proof. Let $K^{-1}(v_i, v_j(n, m))(u, x)$ denote $K^{-1}(v_i, v_j(n, m))$ with parameters u and x , where $i, j \in \{3, 4\}$. By following the techniques in the proof of Theorem 5 and only computing the integral with respect to w gives

$$(3.36) \quad K^{-1}(v_i, v_j(n, m))(1/(ux^2), x) = (-1)^{n+m} K^{-1}(v_i, v_j(n, m))(u, x).$$

In other words, we have an two integrals with respect to v which differ by a factor of $(-1)^{n+m}$. Taking the Pfaffian of the matrix whose entries are given by the required inverse Kastelyn entries gives the required result (the factor $(-1)^{n+m}$ always affects an even number of rows and columns). \square

4. $u < u_c$ (NOT DEPENDENT ON x):

In this section, we prove Theorem 2 using a sequence of lemmas and propositions. These lemmas and propositions lead to the following informal description of the model. Before re-scaling, particles are created in pairs and the probability of survival of these particles decays exponentially with time. It is not unreasonable to expect that the particle model only consists of loops. The interactions between each of these loops can be shown decay

exponentially with distance and with time. Under any scaling window (x, x) each loop contracts to a point and the distribution of these points is a Poisson point process with intensity $u^2(1/\sqrt{1-4u^2} - 1)$ as given in Theorem 2. Figure 8 shows a realization of the particle model for $u < u_c$.

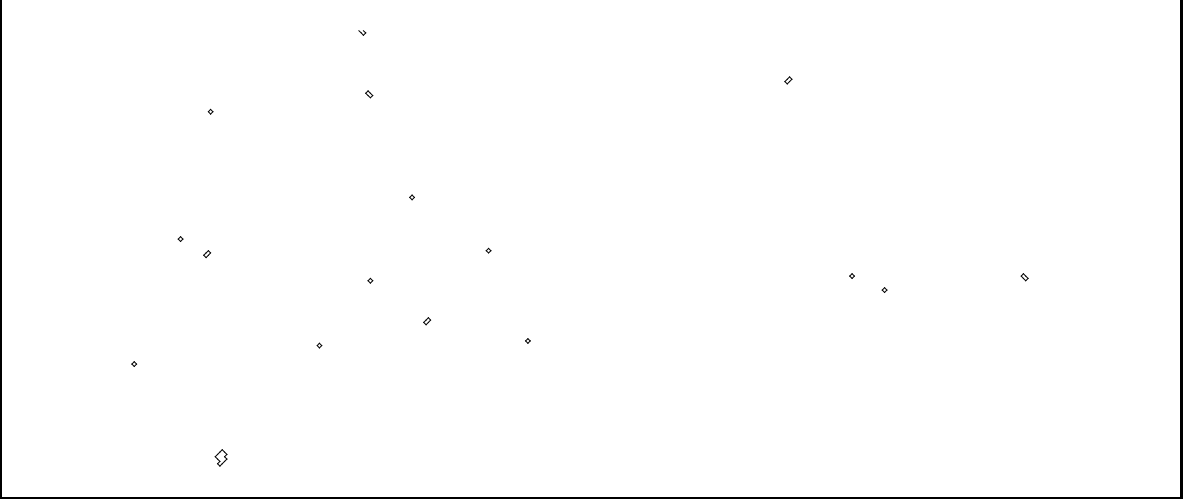


Figure 8: A simulation of the particle model on a grid of 100 by 100, with $u = 0.4$ and $x = 0.1$ using Glauber dynamics

Before embarking on stating and proving the lemmas and propositions, we first introduce and recall some notation. Recall that $v_1(m, n), \dots, v_6(m, n)$ represent the vertices in the fundamental domain (m, n) and that the fundamental domain (m, n) is the fundamental domain at $(0, 0)$ translated by $(m + n, m - n) \in \mathbb{Z}^2$. Define $X(m, n)$ to be the event of observing the leftward upward \mathbf{b} dimer leaving the fundamental domain (m, n) (i.e. the event of seeing a dimer covering the edge from $v_6(m, n)$ to $v_1(m + 1, n)$). The inverse Kastelyn entries for vertices in different fundamental domains requires Fourier coefficients of $P(z, w)$ denoted by $H(m, n)$. In other words,

$$(4.1) \quad H(m, n) = \frac{1}{(2\pi i)^2} \int_{|z|=1} \int_{|w|=1} \frac{z^m w^n}{P(z, w)} \frac{dz}{z} \frac{dw}{w}.$$

The next lemma gives $H(m, n)$ as an expansion in terms of x .

Lemma 8. *Let r_1 and r_2 be the roots of the polynomial $u + w + uw^2$ with $|r_1| < 1$ and $|r_2| > 1$ and set $s_1 = u/(u + r_1)$ and $s_2 = u/(u + r_2)$. Then, for $n, m \geq 1$,*

$$(4.2) \quad H(m, n) = \frac{(-u)^{m+n}(m+n)!}{u(r_1 - r_2)} \left(\frac{{}_2F_1(1, -m, 1+n, s_1^{-1})}{m!n!} - s_2 \sum_{k=0}^{n-1} \frac{(-s_2)^{n-1-k}}{k!(m+n-k)!} \right) + O(x)$$

where ${}_2F_1$ is the confluent hypergeometric function of the second kind.

Proof. By letting

$$(4.3) \quad \tilde{P}(z, w) = \lim_{x \rightarrow 0} \frac{1}{x^2} zw \det K(z, w) = (1 + zu + wu)(wz + uz + uw)$$

then using the analysis of the roots in Section 3.3, by the Dominated Convergence theorem, we can take series expansion in terms of x , which yields

$$(4.4) \quad H(m, n) = \frac{1}{(2\pi i)^2} \int_{|z|=1} \int_{|w|=1} \frac{z^m w^n}{\tilde{P}(z, w)} dz dw + O(x).$$

As $|uw|/|u+w| < 1$ for all $|w| = 1$, then using the factorization of $\tilde{P}(z, w)$ in (4.3) gives

$$(4.5) \quad H(m, n) = \frac{1}{2\pi i} \int_{|w|=1} \left(-\frac{uw}{u+w} \right)^n \frac{w^m}{u+w+uw^2} dw.$$

Notice that

$$(4.6) \quad u+w+uw^2 = \frac{1}{u(r_1-r_2)} \left(\frac{1}{w-r_1} - \frac{1}{w-r_2} \right)$$

As $|r_1| < 1$, the contribution for (4.5) obtained by deforming the contour of integration to $|w-r_1| = \epsilon$ is given by

$$(4.7) \quad \frac{(-u)^n r_1^{m+n}}{u(r_2-r_1)(r_1+u)^n}.$$

The remaining contribution for (4.5) comes from deforming the contour of integration to $|w+u| = \epsilon$. For $v \in \mathbb{C}$ with $v \neq u$, notice that

$$(4.8) \quad \frac{1}{2\pi i} \int_{|w+u|=\epsilon} \left(-\frac{uw}{u+w} \right)^n \frac{w^m}{w+v} dw = (-u)^{m+n} (m+n)! \sum_{k=0}^{n-1} \frac{(-1)^{n-k-1}}{k!(m+n-k)!} \left(\frac{u}{u-v} \right)^{n-k}$$

$$(4.9) \quad = -(-1)^m \left(-\frac{u}{u-v} \right)^n v^{m+n}$$

$$(4.10) \quad -(-u)^{m+n} \frac{(m+n)!}{m!n!} {}_2F_1(1, -m, 1+n, 1-v/u)$$

Substituting in the desired values of v and manipulating gives the desired result. \square

From the above lemma, we can compute the asymptotic expansion of $H(m, n)$ for $m, n > 0$. Let $m = n + k$, then

$$(4.11) \quad H(n+k, n) = \frac{(-u)^{2n+k} (2n+k)!}{(n+k)!n!} + O(u^{2n+k+1})$$

We also require $H(-m, n)$ or $H(m, -n)$ for $m, n \geq 1$, which is given below.

Lemma 9. For $m, n \geq 1$, then

$$(4.12) \quad H(-m, n) = (-1)^{n+m} \left(\frac{1 - \sqrt{1-4u^2}}{2u} \right)^{n+m} + O(x).$$

Proof. Without loss of generality, suppose that $n \geq m$. Taking the series expansion about $x = 0$ gives

$$(4.13) \quad H(-m, n) = \frac{1}{(2\pi i)^2} \int_{|w|=1} \int_{|z|=1} \frac{w^n}{z^m (1+zu+wu)(uw+uz+wz)} dz dw + O(x)$$

By noticing that

$$(4.14) \quad \frac{1}{(1+zu+wu)(uw+uz+wz)} = \frac{1}{u+w+uw^2} \left(\frac{u+w}{uw+uz+wz} - \frac{u}{1+uw+uz} \right)$$

then completing the residue calculations with respect to z leads to the simplification

$$(4.15) \quad H(-m, n) = \frac{1}{2\pi i} \int_{|w|=1} \frac{(-1)^m u^m w^n}{(u+w+uw^2)(1+uw)^m} dw + O(x)$$

$$(4.16) \quad = \frac{(-1)^m u^m r_1^n}{(1+ur_1)^m \sqrt{1-4u^2}} + O(x)$$

where r_1 is the root lying inside of the unit circle of the polynomial $u+w+uw^2$. Simplifying the above equation gives the result. \square

It is clear that for $u < 1/2$, then $H(m, n)$ decays exponentially. This leads to the following proposition:

Proposition 1. For $m, n \in \mathbb{Z}$ and $|m| > |n|$ with $k = ||m| - |n||$.

$$(4.17) \quad \mathbb{P}(X(0, 0), X(m, n)) = 4u^4 x^4 \left(1 - \frac{1}{\sqrt{1-4u^2}} \right)^2 + Cx^2(-u)^{4n+2k} + O(u^{4n+2k+1})$$

where C is an arbitrary constant.

Proof. We only compute the result for $m > n > 1$ as the other cases follow from very similar calculations. Using the local statistics formula (2.7), $\mathbb{P}(X(0, 0), X(m, n))$ is given by

$$(4.18) \quad u^2 x^2 \text{Pf} \begin{pmatrix} 0 & K^{-1}(v_6, v_1(-1, 0)) & K^{-1}(v_6, v_6(-m, -n)) & K^{-1}(v_6, v_1(-m+1, -n)) \\ \cdots & 0 & K^{-1}(v_1, v_6(-m-1, -n)) & K^{-1}(v_1, v_1(-m, -n)) \\ \cdots & \cdots & 0 & K^{-1}(v_6, v_1(-1, 0)) \\ \cdots & \cdots & \cdots & 0 \end{pmatrix}$$

Two of the interaction terms can be computed directly using Lemma 8 by noticing that

$$(4.19) \quad K^{-1}(v_6, v_6(-m, -n)) = -K^{-1}(v_1, v_1(-m, -n)) = -uH(m-1, n) + uH(m+1, n)$$

It still remains to find $K^{-1}(v_1, v_6(-m-1, -n))$ and $K^{-1}(v_6, v_1(-m+1, -n))$. Notice that

$$(4.20) \quad K^{-1}(v_6, v_1(-m+1, -n)) = \frac{1}{x(2\pi i)^2} \int_{|z|=1} \int_{|w|=1} \frac{z^{m-1} w^n}{uw+uz+wz} dw dz + O(1)$$

$$(4.21) \quad = \frac{(m+n-1)!}{x(m)!(n-1)!} (-u)^{m+n-1} + O(1).$$

The remaining interaction entry, $K^{-1}(v_1, v_6(-m-1, -n))$, contains terms of the form

$$(4.22) \quad I(m, n) = \frac{x}{(2\pi i)^2} \int_{|z|=1} \int_{|w|=1} \frac{z^n w^m}{(uw+uz+wz)(1+uz+uw)^2} dw dz$$

$I(m, n)$ can be computed by differentiating $H(m, n)$ by r_1 and r_2 . However, this leaves a contribution of $O(u^{2n+k+1})$. Combining all the linear terms of $I(m, n)$ and multiplying by $K^{-1}(v_6, v_6(-m, -n))$ contributes a maximum of $O(u^{4n+2k+1})$, and so is absorbed into $O(u^{4n+2k+1})$.

The term $K^{-1}(v_6, v_1(1, 1))$ can be computed via residue calculations, which gives

$$(4.23) \quad ux \left(1 - \frac{1}{\sqrt{1 - 4u^2}} \right)$$

Putting together the various contributions gives the result. \square

Proposition 1 can be generalized to show that the difference between the joint probability for k edges and the product of the probabilities of each edge is an exponentially decaying term. This can be achieved by using a complete graph representation of the Pfaffian and ignoring the matchings which contain exponentially decaying weighted edges. For brevity, we omit the details.

Let A_n be the event of seeing a string of \mathbf{b} edges crossing an n by n square. This corresponds to seeing a particle traversing an n by n square in the particle model. Then

Proposition 2.

$$(4.24) \quad \mathbb{P}(A_n) \leq Ce^{-Bn}$$

where B and C are positive constants.

Proof. The event A_n is contained in the event of seeing two \mathbf{b} edges at the top and bottom of the n by n square at any position. Therefore

$$(4.25) \quad \mathbb{P}(A_n) \leq n^2 \sup_k \mathbb{P}(X(0, 0) \cap X(n - k, k))$$

By a symmetrical consideration, the maximal probability occurs when the two \mathbf{b} edges are vertical, i.e. when $k = n/2$. Using Proposition 1 gives

$$(4.26) \quad \mathbb{P}(A_n) \leq n^2 \left(u^4 x^4 \left(1 - \frac{1}{\sqrt{1 - 4u^2}} \right) + Cx^2(-u)^{2n} \right)$$

Taking $n \sim -\log x$ shows that $\mathbb{P}(A_n)$ decays exponentially with distance. \square

The above lemmas and propositions enables the proof of Theorem 2.

Proof of Theorem 2. By Proposition 2, each loop generated by a string of \mathbf{b} edges is finite and does not appear in the scaling window by (x, x) almost surely. Therefore, each loop of \mathbf{b} edges will be contracted to a single point under re-scaling. Tightness is guaranteed for point processes (see [DVJ88]). It is enough to consider the locations of \mathbf{b} edges and show that the finite dimensional distributions of the corresponding measures converge in the scaling window (x, x) . We shall follow the approach developed in the proof of Theorem 4 for the case $u = u_c$ (see Section 5.2) and use the corresponding multi-index notation.

Let \mathbb{P}_x denote the point process in \mathbb{R}^2 arising from the location of a single \mathbf{b} edge in a loop. Let A_i , for $i \in \{1, \dots, k\}$, be disjoint, non-empty simply connected domains and let \tilde{A}_i be the union of lattice points in $((2\mathbb{Z} \times 2\mathbb{Z}) \cup ((2\mathbb{Z} + 1) \times ((2\mathbb{Z} + 1)))$ so that $x\tilde{A}_i \rightarrow A_i$ as $x \rightarrow 0$. For $n \in \mathbb{N}_0^k$, then

$$(4.27) \quad \mathbb{E}_x \left[\prod_{j=1}^k \frac{N(A_j)!}{(N(A_j) - n_j)!} \right] = \sum_{(i_1, t_1) \in \tilde{A}_1} \cdots \sum_{(i_{|n|}, t_{|n|}) \in \tilde{A}_k} \mathbb{P}(X(i_1, t_1), \dots, X(i_{|n|}, t_{|n|})).$$

As each edge is separated by a distance of at least $1/x$, then each of the interaction terms in the inverse Kastelyn matrix converges to zero due to the exponential convergence. Hence,

taking the above limit as $x \rightarrow 0$ gives

$$(4.28) \quad \int_{(A_1)^{n_1}} \cdots \int_{(A_k)^{n_k}} u^{2|n|} \left(\frac{1}{\sqrt{1-4u^2-1}} \right)^{|n|} dx_1^{n_1} \cdots dx_k^{n_k}.$$

Let

$$(4.29) \quad Q_x(z) = \sum_{p \in \mathbb{N}_0^k} \frac{(-z)^p}{p!} \mathbb{E}_x \left[\prod_{j=1}^k \frac{N(A_j)!}{(N(A_j) - p_j)!} \right]$$

and set

$$(4.30) \quad Q_0(z) = \sum_{p \in \mathbb{N}_0^k} \frac{(-z)^p}{p!} \int_{(A_1)^{n_1}} \cdots \int_{(A_k)^{n_k}} u^{2|n|} \left(\frac{1}{\sqrt{1-4u^2-1}} \right)^{|n|} dx_1^{n_1} \cdots dx_k^{n_k}$$

i.e. a generating function for a Poisson point process. Notice that each generating function can also be written as a power series whose coefficients are given by the finite dimensional distribution probabilities for the corresponding measure on the sets A_1, \dots, A_m . Following the same convergence argument given in the proof of Theorem 4 for $u = u_c$, then it is clear that the derivatives of $Q_x(z)$ (with respect to z) converge to $Q_0(z)$. This proves the convergence of finite dimensional distributions. \square

5. THE PARTICLE MODEL FOR $u = u_c$

This section focuses on the critical case in which $u = u_c = \frac{-1+\sqrt{1+x^2}}{x^2}$. Recall that a dimer model is said to be critical if $P(z, w) = 0$ for some $(z, w) \in \mathbb{T}^2$. Moreover, it can be shown that the values of (z, w) , which gives $P(z, w) = 0$, must be real (see [BdT08]). We first look at the local dynamics in the thermodynamic limit. This allows us to produce random walk type estimates that are required later. We can then prove Theorem 4 for $u = u_c$ (or $\gamma = -1$) by obtaining the appropriate correlation kernel in the scaling window (x, x^2) . Finally, using the random walk estimates, we can determine that the set of creations in the scaling window leading to ‘non-trivial paths’ (paths of length greater than $\epsilon > 0$ in the scaling window) is a locally finite Poisson point process. Figure 9 shows a simulation of the particle model for $x = 0.1$ and $u = u_c$.

Our constraints for the choice of scaling window is that it satisfies Donsker’s scaling (i.e. scaling space by the square root of time) and gives non-trivial paths. We choose to take the scaling window (x, x^2) by the following argument: Suppose we choose the scaling window $(x^\alpha, x^{2\alpha})$. It suffices to look at the expected number of dimers covering \mathbf{b} edges in a box of size $(x^{-\alpha}, x^{-2\alpha})$. By Lemma 5, this is $\Theta(x^{1-3\alpha})$. The only value of α that ensures that we see non-trivial paths (i.e. expected number of dimers covering \mathbf{b} edges is $x^{-2\alpha}$ in the box of size $(x^{-\alpha}, x^{-2\alpha})$) is $\alpha = 1$.

5.1. Local Dynamics. This section concentrates on computing random walk estimates of the particles in the particle model for $u = u_c$. These estimates rely on computing the entries of an appropriate inverse Kastelyn matrix. The following lemma provides the underlying entries of the inverse Kastelyn entries.

Lemma 10. *For $m \geq n$ and $m = o(1/x)$*

$$(5.1) \quad \frac{1}{(2\pi i)^2} \int_{|w|=1} \int_{|z|=1} \frac{z^m w^{-n} - (-1)^{m-n}}{P(z, w)} \frac{dz}{z} \frac{dw}{w} = F_0(m, n) + F_1(m, n) + F_2(m, n) + F_3(m, n) + O(x^4)$$

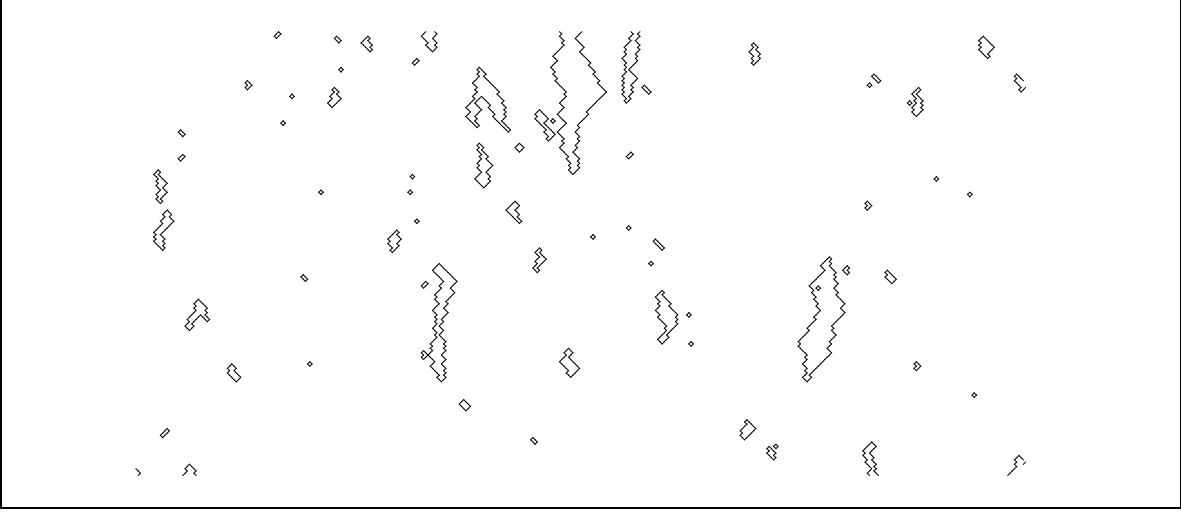


Figure 9: A simulation of the particle model on a 100 by 100 grid with $u = u_c$ and $x = 0.1$ made using Glauber dynamics.

where

$$(5.2) \quad F_0(m, n) = (-1)^{m-n}(m+n),$$

$$(5.3) \quad F_1(m, n) = \frac{2(-1)^{m-n}(m+n)^2x}{\pi}$$

$$(5.4) \quad F_2(m, n) = -\frac{1}{6}(-1)^{m-n}(m+n)(1+2m^2+4mn+2n^2)x^2$$

and

$$(5.5) \quad F_3(m, n) = \frac{(-1)^{m-n}}{9\pi}(m+n)(-7-20m^2+12m^4+200mn+48m^3n-20n^2+72m^2n^2+48mn^3+12n^4)x^3$$

The expansion does hold for $n \geq m$. The $(-1)^{m-n}$ is required so that the above integral converges (due to having a singularity at $z = w = -1$ as $P(-1, -1) = 0$). The lower order terms are required for later computations involving the random walk estimates.

Proof. The first integral can be computed via a residue calculation, leaving

$$(5.6) \quad \frac{1}{2\pi i} \int_{|w|=1} \frac{x^4 \left(-(-1)^{m-n} + w^{-n} \left(-\frac{1+w^2+w(3+x^2)-\sqrt{(1+w)^2(1+2w+w^2+4wx^2)}}{1+2w-x^2} \right)^m \right)}{2 \left(2+x^2-2\sqrt{1+x^2} \right) \sqrt{(1+w)^2(1+w^2+w(2+4x^2))}} dw$$

Note that there is a branch cut situated along the negative real axis from $1-2x^2-2x\sqrt{1+x^2}$ to $r = -1-2x^2+2x\sqrt{1+x^2}$. Therefore, the integral over $|w|=1$ in (5.6) can be deformed to an integral from $w = -1$ to $w = r$ (above the branch cut), an integral from $w = r$ to $w = -1$ (below the branch cut) and a contour integral around $w = \frac{1}{2}(x^2-1)$.

The contributions given near the branch cut can be computed in a very similar fashion as follows. By taking a series expansion of the numerator about the point $w = -1$ gives an integral of the following form

$$(5.7) \quad \frac{1}{2\pi i} \int_{-1}^r \frac{x^4}{2(2+x^2-2\sqrt{1+x^2})} \sum_{k=0}^{\infty} a_k \frac{(w+1)^{k+1}}{\sqrt{(w+1)^2(1+w^2+w(2+4x^2))}} dw$$

where a_k is a function of m, n and x . Each of the integrals

$$(5.8) \quad I_i := 1/(2\pi i) \int_{-1}^r \frac{(w+1)^{i-1}}{\sqrt{(w+1)^2+4wx^2}} dw$$

can be evaluated. It suffices to only compute I_i up to $i = 5$ as $I_i = O(x^{i-1})$ and each a_k is $O(1)$. Summing up the contribution near the branch cut gives

$$-F_0(m, n) + F_1(m, n) - F_2(m, n)x^2 + F_3(m, n)x^3.$$

It remains to calculate the other contribution in (5.6), namely the contour integral around $w = \frac{1}{2}(x^2 - 1)$. Taking a series expansion in x gives

$$(5.9) \quad \frac{1}{2\pi i} \int_{|w+\frac{1}{2}|=\epsilon} \frac{2(-1)^m w^{m-n}}{(1+2w)^m(1+w)^2} - \frac{2((-1)^m w^{1+m-n} (1+2w+m(1+w)^2)) x^2}{(1+2w)^{m+1}(1+w)^4} dw + O(x^4).$$

This can be computed using the following integral

$$(5.10) \quad G(l) =: \frac{1}{2\pi i} \int_{|w+\frac{1}{2}|=\epsilon} \frac{w^{m-n}}{(1+2w)^m(1+w)^l} dw$$

These can all be found by a higher dimensional residue formula and are given by $G(1) = (-1)^n$, $G(2) = (-1)^n(m+n)$

$$(5.11) \quad G(3) = \frac{1}{2}(-1)^n(-2+m^2+n+n^2+m(3+2n))$$

and

$$(5.12) \quad G(4) = \frac{1}{6}(-1)^n(2+m+n)(-6+m^2+n+n^2+m(7+2n)).$$

Adding up the various contributions gives the result. \square

Recall that $v_i(n, m)$ denote the vertex v_i in the (n, m) fundamental domain. For $(y, t) \in (\mathbb{Z} \times \mathbb{Z}) \cup ((2\mathbb{Z}+1) \times (2\mathbb{Z}+1))$, let $X(y, t)$ denote the event that there is a particle at (y, t) where we think of y as space and t as time. Note that $\mathbb{P}(X(y, t)) = 1 - \mathbb{P}(\text{'a' edge}) = 1 - xK^{-1}(3, 4)$.

Proposition 3. *The covariance of two particles a distance n away with $n = o(1/x)$, is given by*

$$(5.13) \quad \mathbb{P}(X(0, t), X(n, t)) = \left(1 - \frac{4}{\pi^2}\right) x^2 - \frac{8n}{\pi} x^3 + O(x^4)$$

Proof. The proof of this proposition is a calculation using the inclusion exclusion formula given in Lemma 3. The interaction entries, $K^{-1}(v_3, v_3(n, -n))$ and $K^{-1}(v_3, v_4(n, -n))$, can be calculated as an expansion using Lemma 10

$$(5.14) \quad K_{n,-n}^{-1}(v_3, v_3(n, -n)) = 1 - \frac{8nx}{\pi} + (1+4n^2)x^2 - \frac{4(-3+34n+32n^3)x^3}{9\pi}$$

and

$$(5.15) \quad K_{n,-n}^{-1}(v_3, v_4(n, -n)) = \frac{2}{\pi} - 2nx + \frac{(10+8n)x^2}{3\pi} - 3nx^3.$$

In Section 3, we computed $1 - xK^{-1}(v_3, v_4)$. Plugging the required entries into the appropriate Pfaffian gives the required result. \square

The local dynamics of the particles can also be computed. This entails the conditional distribution of two particles separated by a distance n .

Proposition 4. *For two particles separated by a distance $n = o(1/x)$, then*

- $\mathbb{P}[X(1, t+1), X(n-1, t+1) | X(0, t), X(n, t)] = \frac{1}{4} + \frac{x}{\pi} + O(x^2)$
- $\mathbb{P}[(X(-1, t+1), X(n+1, t+1) | X(0, t), X(n, t)] = \frac{1}{4} - \frac{x}{\pi} + O(x^2)$
- $\mathbb{P}[(X(-1, t+1), X(n-1, t+1) | X(0, t), X(n, t)] = \frac{1}{4} + O(x^2)$
- $\mathbb{P}[(X(1, t+1), X(n+1, t+1) | X(0, t), X(n, t)] = \frac{1}{4} + O(x^2)$

Proof. The existence of particles at $X(0, t)$ and $X(n, t)$ means no dimers covering **a** edges at those locations. Thus, the dynamics of the particles are governed by the locations of dimers on the inverted triangle decoration. Therefore, the probability that there are particles at $X(0, t)$ and $X(n, t)$ and they move closer together is given by,

$$(5.16) \quad \text{Pf} \begin{pmatrix} 0 & K^{-1}(v_4, v_6) & K_{n,-n}^{-1}(v_4, v_4(n, -n)) & K_{n,-n}^{-1}(v_4, v_5(n, -n)) \\ \dots & 0 & K_{n,-n}^{-1}(v_6, v_4(n, -n)) & K_{n,-n}^{-1}(v_6, v_5(n, -n)) \\ \dots & \dots & 0 & K^{-1}(v_4, v_5) \\ \dots & \dots & \dots & 0 \end{pmatrix} = x^2/4 - \frac{2nx^3}{\pi} + O(x^4)$$

where $K_{n,-n}^{-1}(v_*, v_*(n, -n))$ has been computed using Lemma 10. To compute the conditional probability that the particles move together given that there are two particles, it suffices to divide (5.16) by the joint probability of seeing two particles separated by distance n . This gives $1/4 + x/\pi$. The other quantities can be computed in a similar fashion. \square

5.2. Location of particles in the scaling window. This subsection concentrates on finding the measure for the locations of particles along a horizontal line in the scaling window (x, x^2) for $u = u_c$. In particular, we prove Theorem 4 in the special case when $u = u_c$ or $\gamma = -1$.

The proof of this theorem follows by a sequence of lemmas and propositions. Recall that $v_i(n, m)$ is the vertex v_i in the (n, m) fundamental domain. In order to prove the above theorem, we need to find the entries of the inverse Kastelyn matrix in the re-scaling. This relies on the following:

Lemma 11. *Suppose that $nx = \alpha$ where $\alpha \in [0, \infty)$. Then,*

$$(5.17) \quad K^{-1}(v_3, v_3(n, -n)) = E_1(\alpha) + O(x^2)$$

Furthermore,

$$(5.18) \quad K^{-1}(v_3, v_4(n, -n)) = E_2(\alpha) + E_3(\alpha)x + O(x^2)$$

where $E_1(\alpha), E_2(\alpha)$ are defined in Theorem 4 and

$$(5.19) \quad E_3(\alpha) = \frac{2}{\alpha\pi} - 4B_I(2, 4\alpha) + 4S_L(-2, 4\alpha)$$

where $B_I(n, z)$ stands for the modified Bessel function of the first kind and $S_L(n, z)$ denotes the modified Struve Function.

The calculation is only given for $K^{-1}(v_3, v_3(n, -n))$ as the other term is analogous and can be completed with exactly the same steps.

Proof. The first entry is given by

$$(5.20) \quad K^{-1}(v_3, v_3(n, -n)) = \frac{1}{(2\pi i)^2} \int_{\mathbb{T}^2} \frac{w^{-1-n} z^{n-1} (-w^2 + z^2)}{(z - y_1)(z - y_2)(1 + 2w - x^2)} dz dw.$$

A residue can be taken with respect to z at y_2 due to $|y_2(w)| < 1$ for all $|w| = 1$. This results in an integrand containing the term $\sqrt{(1+w)^2 + 4wx^2}$ in both the numerator and the denominator. To rewrite the integrand without this square root term, set $x = 1/2\sqrt{-2 - 1/r - r}$ and take the change of variables $w = (r - u^2)/(1 - u^2r)$. The transformation changes the contour of integration to a unit semi-circle from -1 to 1 passing through the point $-i$. This contour shall be denoted C_1 . Note that r is the root of $(1+w)^2 + 4wx^2$ whose absolute value is less than 1. Finally, setting $R^2 = r$ gives

$$(5.21) \quad K^{-1}(v_3, v_3(n, -n)) = \frac{1}{2\pi i} \int_{C_1} -\frac{8R^2 (-1 + R^2) (R - u)(-1 + Ru)}{(R + u)(1 + Ru)(-1 - 3R^2 + R(3 + R^2)u)} f(w) dw$$

where

$$(5.22) \quad f(w) = \left(\frac{(R - u)(3R + R^3 - u - 3R^2u)}{(-1 + Ru)(-1 - 3R^2 + 3Ru + R^3u)} \right)^n \frac{1}{(-u + R(3 + R^2 - 3Ru))}.$$

The transformation, $u = \frac{-t+R}{-1+tR}$, moves the contour C_1 to a unit semi-circle from 1 to -1 passing through i . Denote this new contour by C_2 . Then, setting $c_x = -(4R + 4R^3)/(1 + 6R^2 + R^4)$ gives

$$(5.23) \quad K^{-1}(v_3, v_3(n, -n)) = \frac{8R^2}{2\pi i} \int_{C_2} \frac{(1 + R^2 - 2Rt)(t + R(-2 + Rt))(c_x + t)^{n-1}}{(1 + 6R^2 + R^4)^2 t^{n-1} (c_x t + 1)^{1+n}} dt.$$

Setting $n = \alpha/x$ we can take a series expansion of the integrand in (5.23). This gives

$$(5.24) \quad \left(\frac{2e^{-(2i\alpha)/t+2i\alpha t}}{t} \right) \left(1 + x \frac{(1 + t^2)(-2\alpha - it + 2\alpha t^2)}{t^3} \right) + O(x^2)$$

Applying the bounded convergence theorem to (5.23) along with the change of variables $t = e^{i\theta}$ gives

$$(5.25) \quad K^{-1}(v_3, v_3(n, -n)) = \frac{1}{\pi} \int_0^\pi e^{-4\alpha \sin \theta} (1 + 2ix \cos \theta (-1 + 4\alpha \sin \theta)) d\theta + O(x^2)$$

$$(5.26) \quad = \frac{1}{\pi} \int_0^\pi e^{-4\alpha \sin \theta} d\theta + O(x^2)$$

The above integral can be evaluated in terms of the Bessel and Struve functions. □

The proof of Lemma 11 also shows the ‘correct’ horizontal scaling. This can be shown by the series expansion of integrand in (5.23). Taking a larger scaling, i.e. for $\epsilon > 0$ set $n = \alpha/x^{1+\epsilon}$, leads to (5.23) converging to zero. Taking a smaller scaling, i.e. set $n = \alpha/x^{1-\epsilon}$, then (5.23) converges to 1 as $x \rightarrow 0$. In essence, $n = \alpha/x$ provides the right horizontal scaling to ensure decay of the inverse Kastelyn entry.

For $1 \leq i \leq m$, let $x_i \in x\mathbb{Z} \subset \mathbb{R}$ denote possible particle locations on the lattice $x\mathbb{Z}$. Let $\rho_x^m(x_1, \dots, x_m)$ denote the m point correlation function of seeing particles at (x_1, \dots, x_m) with the corresponding measure on \mathbb{R} denoted by $\mathbb{P}_x^{u_c}$, then

Proposition 5. *The m -point correlation function for the re-scaled particle locations, $\rho_m(y_1, \dots, y_m)$ is given by*

$$(5.27) \quad \rho_m^x(x_1, \dots, x_m) = \text{Pf} \left(M_{u_c, x}^{res}(x_i, x_j) \right)_{i,j=1}^m + O(x^{2m+2})$$

where $M_{u_c, x}^{res}$ is antisymmetric matrix with

$$(5.28) \quad M_{u_c, x}^{res}(x_i, x_i) = \begin{pmatrix} 0 & \frac{2}{\pi}x - x^2 \\ -\frac{2}{\pi}x + x^2 & 0 \end{pmatrix}$$

and

$$(5.29) \quad M_{u_c, x}^{res}(x_i, x_j) = \begin{pmatrix} -xE_1(|x_j - x_i|) & -xE_2(|x_j - x_i|) - xE_3(|x_j - x_i|) \\ xE_2(|x_j - x_i|) + xE_3(|x_j - x_i|) & xE_1(|x_j - x_i|) \end{pmatrix}.$$

where $E_1(\alpha), E_2(\alpha)$ and $E_3(\alpha)$ are defined in Lemma 11

Proof of Proposition 5. This is a direct consequence of Lemma 11 and the underlying Pfaffian structure of computing the probability of the location of m particles on this particular dimer model. \square

The above calculations provide a proof for Theorem 4 for the case $u = u_c$. The proof follows an argument from [Bou07].

Proof of Theorem 4 for $u = u_c$. Notice that as $\mathbb{P}_x^{u_c}$ and $\mathbb{P}_0^{u_c}$ are both defined in the same space of measures, then it is enough to prove that $\mathbb{P}_x^{u_c}$ converges weakly to $\mathbb{P}_0^{u_c}$. Due to considering point processes, then tightness of the measures is guaranteed (see [DVJ88]), so it remains to show convergence of finite dimensional distributions. Let $N(\cdot)$ denote number of particles in a set, $\{A_1, \dots, A_k\}$ denote a family of disjoint Borel sets in \mathbb{R} and $n_1, \dots, n_k \in \mathbb{N}_0$, then we need to show

$$(5.30) \quad \lim_{x \rightarrow 0} \mathbb{P}_x^{u_c}(N(A_1) = n_1, \dots, N(A_k) = n_k) = \mathbb{P}_0^{u_c}(N(A_1) = n_1, \dots, N(A_k) = n_k)$$

In order to prove such an equality, we need to write the measures $\mathbb{P}_x^{u_c}$ and $\mathbb{P}_0^{u_c}$ in terms of their m -point correlation functions, which can be achieved by writing their respective generating functions. Denote $n! = \prod_{j=1}^k n_j!$, $|n| = \sum_{j=1}^k n_j$, $z = (z_1, \dots, z_k)$ and $z^n = z_1^{n_1} \dots z_k^{n_k}$. The Taylor series of the generating function of $\mathbb{P}_x^{u_c}$ about the point $z = 0$ is

$$(5.31) \quad Q_x(z) = \mathbb{E}_x \left[\prod_{j=1}^k (1 - z_j)^{N(A_j)!} \right]$$

$$(5.32) \quad = \sum_{p \in \mathbb{N}_0^k} \frac{(-z)^p}{p!} \mathbb{E}_x \left[\prod_{j=1}^k \frac{N(A_j)!}{(N(A_j) - p_j)!} \right]$$

$Q_x(z)$ can also be expressed as a power series with coefficients z^n given by $\mathbb{P}_x^{u_c}(N(A_1) = n_1, \dots, N(A_k) = n_k)$. The two representations of the generating function give

$$(5.33) \quad \mathbb{P}_x^{u_c}(N(A_1) = n_1, \dots, N(A_k) = n_k) = \frac{(-1)^n}{n!} \frac{\partial^n}{\partial z^n} Q_x(z) \Big|_{z=(1, \dots, 1)}$$

Similarly, the generating function of $\mathbb{P}_x^{u_c}$ is given by

$$(5.34) \quad Q_0(z) = \sum_{p \in \mathbb{N}_0^k} \frac{(-z)^p}{p!} \mathbb{E}_0 \left[\prod_{j=1}^k \frac{N(A_j)!}{(N(A_j) - p_j)!} \right].$$

Therefore, (5.30) is equivalent to showing

$$(5.35) \quad \lim_{x \rightarrow 0} \frac{\partial^n}{\partial z^n} \frac{(-1)^n}{n!} Q_x(z) \Big|_{z=(1, \dots, 1)} = \frac{\partial^n}{\partial z^n} \frac{(-1)^n}{n!} Q_0(z) \Big|_{z=(1, \dots, 1)}.$$

Without loss of generality, suppose that the family of Borel sets, $\{A_1, \dots, A_k\}$ is open. Let $\tilde{A} = \{y \in \mathbb{Z} : yx \in A\}$ for any set open set A . Using Proposition 5 gives

$$(5.36) \quad \mathbb{E}_x \left[\prod_{j=1}^k \frac{N(A_j)!}{(N(A_j) - n_j)!} \right] = \sum_{x_1 \in x\tilde{A}_1, \dots, x_{|n|} \in x\tilde{A}_k} \text{Pf} (M_{u_c, x}^{res}(x_i, x_j))_{i,j=1}^{|n|}$$

Taking the limit in $x \rightarrow 0$, the Riemann sums converge to

$$(5.37) \quad \int_{A_1^{n_1}} \dots \int_{A_k^{n_k}} \text{Pf} (M_{u_c, x}^{res}(y_i, y_j))_{i,j=1}^{|n|} dy_1^{n_1} \dots dy_k^{n_k}$$

which is exactly the m point correlation function for $\mathbb{P}_0^{u_c}$. By noting that all entries of $(M_{u_c, x}^{res}(x_i, x_j))_{i,j=1}^{|n|}$ are uniformly bounded by 1 (using Proposition 5), we can use Hardamard's inequality,

$$(5.38) \quad \left| \mathbb{E}_x \left[\prod_{j=1}^k \frac{N(A_j)!}{(N(A_j) - n_j)!} \right] \right| \leq \prod_{j=1}^k |A_j| (2|n|)^{|n|/2}$$

This implies that $Q_x(z)$ is an absolutely convergent series. For z in a compact set, then by the Lebesgue Dominated Convergence the derivatives of $Q_x(z)$ converge uniformly to $Q_0(z)$ in the limit $x \rightarrow 0$. This completes the proof of convergence of finite dimensional distributions. \square

5.3. The Creation measure for u_c . The creation singularities, under the scaling window (x, x^2) form a dense set of the plane. This can be seen by the fact that the expected number of creation singularities in a box of size (x^{-1}, x^{-2}) is x^{-1} . Here, we will only consider creation singularities which form non-trivial paths in the scaling window (x, x^2) . By non-trivial paths, we mean paths of length $\epsilon > 0$ in the scaling window (x, x^2) . The measure on the set of creations, whose paths are non-trivial, is a locally finite (Lemma 12) Poisson point process (Theorem 6).

Let B be a box in $(2x\mathbb{Z} \times 2x^2\mathbb{Z}) \cup ((2\mathbb{Z} + 1)x \times (2\mathbb{Z} + 1)x^2)$ with corners $(0, 0)$, $(\alpha, 0)$ and $(0, \beta)$ where $0 < \alpha < \infty$ and $0 < \beta < \infty$ are fixed. Let Ξ_B denote the set consisting of all creation points in B for a realization of the underlying dimer covering. For $(y, z) \in \Xi_B$, let $P_l(y, z, t - z)$ and $P_r(y, z, t - z)$ be the locations of the left and right paths emerging from (y, z) at time $t > z$. We use the convention that $P_l(y, z)$ (or $P_r(y, z)$) represents a realization of the left (or right) path starting from $(y, z) \in \Xi_B$ and $|P_l(y, z)|$ (or $|P_r(y, z)|$) denotes the lifetime of the left (or right) path. Set, for a fixed $\epsilon > 0$,

$$(5.39) \quad \Gamma_B^\epsilon = \{(y, z) \in \Xi_B : \min(|P_l(y, z)|, |P_r(y, z)|) \geq \epsilon\},$$

This represents all the creations that create paths of length greater than ϵ in the appropriate scaling window. The following shows that these creations are locally finite and do appear in the scaling window (x, x^2) .

Lemma 12.

$$(5.40) \quad 0 < \lim_{x \rightarrow 0} \mathbb{E} |\Gamma_B^\epsilon| < \infty$$

Proof. Notice that $|\Gamma_B^\epsilon|$ is less than or equal to the number of paths of length ϵ . If $\lim_{x \rightarrow 0} \mathbb{E} |\Gamma_B^\epsilon| = \infty$, then this implies that the expected number of paths in the scaling limit is not locally finite, which is a contradiction. This proves $\lim_{x \rightarrow 0} \mathbb{E} |\Gamma_B^\epsilon| < \infty$.

The inequality $0 < \lim_{x \rightarrow 0} \mathbb{E} |\Gamma_B^\epsilon|$ is more involved and requires the consideration of a random walk approximation. For $(y, z) \in \Gamma_B^\epsilon$, let $X_t = P_r(y, z, t - z) - P_l(y, z, t - z)$, with $X_0 = x$ and let Y_t , with $Y_0 = 1$, be the random walk which has iid increments of 1, 0 and -1 with probability $1/4 - x/\pi$, $1/2$ and $1/4 + x/\pi$. Let \mathbb{P}_r denote the corresponding probability measure for the random walk Y_t started at r . Let $T_0^X = \inf\{t > 0 : X_t = 0\}$ and $T_0^Y = \inf\{t > 0 : Y_t = 0\}$. Then,

Claim 1. *There exists $0 < T < T_0^Y$ such that for $0 < t < T$, X_t stochastically dominates xY_{t/x^2} .*

Note that T is the time of death for the shortest path emerging from $(z, y) \in \Gamma_B^\epsilon$ and $T > 0$ almost surely by definition of Γ_B^ϵ . We are only interested in knowing that the difference of paths dominates a random walk for a strictly positive time.

Proof of Claim. The evolution of each particle is a non Markovian process as each particle's trajectory is determined by the locations of the other particles. Proposition 5 shows that the pairwise force between two particles increases as the distance between the particles decreases. The candidate for the random walk approximation can be obtained from Proposition 4, which is defined by Y_t . Due to Y_t having dynamics related to the maximum attraction between two particles, then the attraction between two paths $P_l(z, y)$ and $P_r(z, y)$ is always bounded by Y_t , which does not matter on the locations of other paths. \square

Define $Y_t(y, z)$ to be independent copies of the walk Y_t , indexed by $(y, z) \in \Xi_B$. Define

$$(5.41) \quad \tilde{\Gamma}_B^\epsilon = \{(y, z) \in \Xi_B : T_0^{Y(y, z)} > \epsilon/x^2\}.$$

Due to paths from other creations can collide, then it is not immediately true that $\mathbb{E}[\Gamma_B^\epsilon] \geq \mathbb{E}[\tilde{\Gamma}_B^\epsilon]$. By Lemma 13, the creation singularities on the $1/x \times 1/x^2$ scale are independent. Therefore, we only need to consider annihilations from paths with different creations that are not seen in the scaling window. For $(y_1, z_1), (y_2, z_2) \in \Xi_B$ with $y_1 < y_2$ and $z_1 < z_2$, then $P_l(y_2, z_2, t - z_1) - P_r(y_1, z_1, t - z_1) < -Y_t$ stochastically. Therefore, we require

$$(5.42) \quad \sum_{k > \epsilon} \mathbb{P}_{k/x}(-Y_{t/x} = 0) = \mathbb{P}_{-1}(Y_{t/x} > -\epsilon/x | Y_r < 0, \forall r)$$

$$(5.43) \quad = O(x^2)$$

which can be obtained by using Chebychev's inequality. Using this, we can bound the number of creations whose paths annihilate paths from other creations. This gives an $O(1)$ bound, and hence, up to first order, $\mathbb{E}[\Gamma_B^\epsilon] \geq \mathbb{E}[\tilde{\Gamma}_B^\epsilon] + O(x)$. This implies that

$$(5.44) \quad \lim_{x \rightarrow 0} \mathbb{E}[\Gamma_B^\epsilon] \geq \lim_{x \rightarrow 0} \mathbb{E}[\tilde{\Gamma}_B^\epsilon]$$

and so the rest of the proof hinges on showing $\lim_{x \rightarrow 0} \mathbb{E}[\tilde{\Gamma}_B] > 0$.

By independence,

$$(5.45) \quad \mathbb{E} \left| \tilde{\Gamma}_B^\epsilon \right| \geq \mathbb{E}[|\Xi_B|] \mathbb{P}_1(T_0^Y > \epsilon/x^2)$$

for some $\epsilon > 0$. Notice that

$$(5.46) \quad \mathbb{E}[|\Xi_B|] = 1/x + O(1).$$

It remains to show that a lower bound for $\mathbb{P}_1(T_0^Y > \epsilon/x^2)$ is $O(x)$. Using Kemperman's formula, then,

$$(5.47) \quad \mathbb{P}_1(T_0^Y > \epsilon/x^2) = \sum_{r > \epsilon/x^2} \frac{1}{2r-1} \mathbb{P}(S_{2r-1} = -1)$$

where $S_k = Y_0 + \dots + Y_k$ and

$$(5.48) \quad \begin{aligned} \mathbb{P}(S_{2r-1} = -1) &= \sum_{k=0}^{2r-1} \binom{2r-1}{k} \binom{2r-1-k}{k+1} \left(\frac{1}{4} + \frac{x}{\pi}\right)^k \left(\frac{1}{4} - \frac{x}{\pi}\right)^{k+1} 2^{-(2r-2-2k)} \\ (5.49) \quad &= \frac{1}{2} \sum_{k=0}^{2r-1} \binom{2r-1}{k} \binom{2r-1-k}{k+1} \left(\frac{1}{4}\right)^k 2^{-(2r-1)} + O(x^2) \end{aligned}$$

Estimating gives

$$(5.50) \quad \mathbb{P}(S_{2r-1} = -1) \geq \sum_{k=[(2r-1)/4]-\sqrt{r}}^{[(2r-1)/4]+\sqrt{r}} \binom{2r-1}{2k+1} \binom{2k+1}{k} \left(\frac{1}{4}\right)^k 2^{-(2r-1)} + O(x^2)$$

$$(5.51) \quad \geq \frac{1}{\sqrt{2r-1}} + O\left(\frac{1}{\sqrt{(2r-1)^3}}\right) + O(x^2)$$

by performing a lower bound estimate on the smallest summand using Stirling's formula. Using the appropriate time re-scaling gives

$$(5.52) \quad \mathbb{P}_1(T_0^Y > \epsilon/x^2) \geq C(\epsilon)x$$

where $C(\epsilon)$ represents some constant dependent on ϵ . Substituting the required components back into (5.45) shows that $\lim_{x \rightarrow 0} \mathbb{E}[\tilde{\Gamma}_B^\epsilon]$ is nontrivial as required. \square

Let $\tilde{B} = \lim_{x \rightarrow 0} B \subset \mathbb{R}^2$. Let X denote the possible locations of creation singularities in B , so that for a dimer covering, X takes values in Ξ_B . Let $\mathbb{P}_{x,\epsilon}^{s,u_c}$ be the point process defined on $\mathcal{B}(\mathbb{R}^2)$, the Borel sets of \mathbb{R}^2 , such that the realization of all the creations whose paths are non-trivial in \tilde{B} is Γ_B^ϵ . Here, the superscript 's' in the measure is to merely indicate singularity. The aim is to show weak convergence of the measure $\mathbb{P}_{x,\epsilon}^{s,u_c}$ to a Poisson point process. Before doing so, we first state and prove a lemma which was used in the proof of Lemma 12 and is used in the proof of Theorem 6.

Lemma 13. *For $k > 0$ and $y_1, \dots, y_k \in B$,*

$$(5.53) \quad \mathbb{P}(X = y_1, \dots, X = y_k) = \prod_{i=1}^k \mathbb{P}(X = y_i) + O(x^{2k+1})$$

Proof. The proof heavily relies on the computation of the asymptotic inverse Kastelyn entries. These can be found algorithmically using a similar method employed in the proof of Lemma 11. The only difference is to take into account the vertical scaling.

It remains to show independence up to a factor of x using the asymptotic inverse Kastelyn entries. Each creation consists of dimers covering edges v_5 to $v_1(1,0)$ and v_6 to $v_2(0,1)$. Notice that

$$(5.54) \quad K^{-1}(v_1(0,1), v_j) = K^{-1}(v_2(1,0), v_j) + O(x)$$

for $j = 5, 6$. For the off diagonal blocks, we have a similar result, namely

$$(5.55) \quad K^{-1}(v_1(0,1), v_j(n, m)) = K^{-1}(v_2(1,0), v_j(n, m)) + O(x)$$

for $j = 5, 6$,

$$(5.56) \quad K^{-1}(v_1(0,1), v_1(n+1, m)) = K^{-1}(v_2(1,0), v_1(n, m+1)) + O(x)$$

and finally

$$(5.57) \quad K^{-1}(v_1(0,1), v_2(n+1, m)) = K^{-1}(v_2(1,0), v_2(n+1, m)) + O(x).$$

This implies that the first two rows (and columns), apart from the 2 by 2 diagonal block, of the underlying inverse Kastelyn matrix $\mathbb{P}(X = y_1, \dots, X = y_k)$, are the same up to $O(x)$. A similar property can be obtained for the third and fourth row. By considering a complete graph representation of the Pfaffian, see [God93], gives

$$(5.58) \quad \mathbb{P}(X = y_1, \dots, X = y_k) = (\mathbb{P}(X = y_1) + O(x^2))\mathbb{P}(X = y_2, \dots, X = y_k)$$

Proceeding by induction gives the result. \square

We can now state and prove a theorem about the locations of creations which give non-trivial paths in the scaling window (x, x^2) .

Theorem 6. *For $\epsilon > 0$, $\mathbb{P}_{x,\epsilon}^{s,u_c}$ converges weakly to a Poisson point process in the limit $x \rightarrow 0$, which has a finite non-zero intensity dependent on ϵ .*

Proof of Theorem 6. The proof follows the same recipe as the proof of Theorem 4 for $u = u_c$ (see Section 5.2). Again, tightness is already guaranteed and we only need to prove convergence of finite dimensional distributions. We borrow the multi-index notation from the proof of Theorem 4 for $u = u_c$.

Let B_1, \dots, B_k represent disjoint boxes in $(2x\mathbb{Z} \times 2x^2\mathbb{Z}) \cup ((2\mathbb{Z} + 1)x \times (2\mathbb{Z} + 1)x^2)$ with \tilde{B}_i representing the box under the limit $x \rightarrow 0$ for $1 \leq i \leq k$. Let f_m denote the m point particle density for Γ_B^ϵ . By Lemma 12, we can write

$$(5.59) \quad \int_{\tilde{B}_1} f_1(y)dy = \lim_{x \rightarrow 0} \sum_{x_1 \in B_1} \mathbb{P}(X = x_1; x_1 \in \Gamma_{B_1}^\epsilon) = \lim_{x \rightarrow 0} \mathbb{E} \left| \bigcup_{t \in \mathbb{Q}_{>0}} A_t^{B_1} \right| < \infty$$

where $\mathbb{P}(\cdot; x_1 \in \Gamma_{B_1}^\epsilon)$ is $\mathbb{P}(\cdot)$ multiplied by the indicator $x_1 \in \Gamma_{B_1}^\epsilon$. Therefore, it is clear that $\mathbb{P}(X = x_1; x_1 \in \Gamma_{B_1}^\epsilon)$ is $O(x^3)$. As the local dimer configurations are translation invariant (due to having zero boundary conditions), then $\int_{\tilde{B}_1} f_1(y)dy = \mu(\tilde{B}_1)\rho$ where ρ is the intensity

of the point process. Using Lemma 13 and convergence of Riemann sums gives

(5.60)

$$\lim_{x \rightarrow 0} \mathbb{E}_{x, \epsilon}^{s, u_c} \left[\prod_{j=1}^k \frac{N(B_j)!}{(N(B_j) - n_j)!} \right] = \lim_{x \rightarrow 0} \sum_{x_1 \in B_1, \dots, x_{|n|} \in B_k} \mathbb{P}(X = x_1; x_1 \in \Gamma_{B_1}^\epsilon, \dots, X = x_{|n|}; x_{|n|} \in \Gamma_{B_{|n|}}^\epsilon)$$

(5.61)

$$= \lim_{x \rightarrow 0} \sum_{x_1 \in B_1, \dots, x_{|n|} \in B_k} \mathbb{P}(X = x_1; x_1 \in \Gamma_{B_1}^\epsilon) \dots \mathbb{P}(X = x_{|n|}; x_{|n|} \in \Gamma_{B_{|n|}}^\epsilon)$$

(5.62)

$$= \left(\int_{\tilde{B}_1} f_1(y) dy \right)^{n_1} \dots \left(\int_{\tilde{B}_1} f_1(y) dy \right)^{n_k}$$

Let

$$(5.63) \quad Q_x(z) = \sum_{p \in \mathbb{N}_0^k} \frac{(-z)^p}{p!} \mathbb{E}_x \left[\prod_{j=1}^k \frac{N(B_j)!}{(N(B_j) - p_j)!} \right]$$

and set

$$(5.64) \quad Q_0(z) = \sum_{p \in \mathbb{N}_0^k} \frac{(-z)^p}{p!} \left(\int_{\tilde{B}_1} f_1(y) dy \right)^{n_1} \dots \left(\int_{\tilde{B}_1} f_1(y) dy \right)^{n_k}$$

i.e. a generating function for a Poisson point process. Notice that each generating function can also be written as a power series whose coefficients are given by the finite dimensional distribution probabilities for the corresponding measure on the sets B_1, \dots, B_m . Following the same convergence argument given in the proof of Theorem 4 for $u = u_c$, then it is clear that the derivatives of $Q_x(z)$ (with respect to z) converge to $Q_0(z)$. This proves the finite dimensional distributions convergence. \square

6. THE PARTICLE MODEL FOR $u = u_i$

In this section, we concentrate on the particle model for $u = u_i$ and prove Theorem 3. The idea behind the proof is to form a bijection with the particle model and the color boundaries of a two color noisy voter model, defined in [GM95]. The weak convergence under the scaling window (x, x^2) is guaranteed by [FINR06], who constructed the scaling window (x, x^2) of the noisy voter model. This limiting object is called the Continuum Noisy Voter Model. Finally, we show that the set of creations which give non-trivial paths in the scaling window (x, x^2) is a locally finite Poisson point process. Figure 9 shows a simulation of the particle model for $x = 0.1$ and $u = u_i$.

6.1. Bijection with the Noisy Voter Model. In this subsection, we show that the particles in the particle model have the same distribution as the boundaries of colors in two colored noisy voter model. This involves showing the distributions of particles are independent Bernoulli random variables, each trajectory is independent and creations are independent.

Let

$$(6.1) \quad H(m, n) = \frac{1}{(2\pi i)^2} \int_{|w|=1} \int_{|z|=1} \frac{z^m}{w^n P(z, w)} \frac{dz}{z} \frac{dw}{w}$$

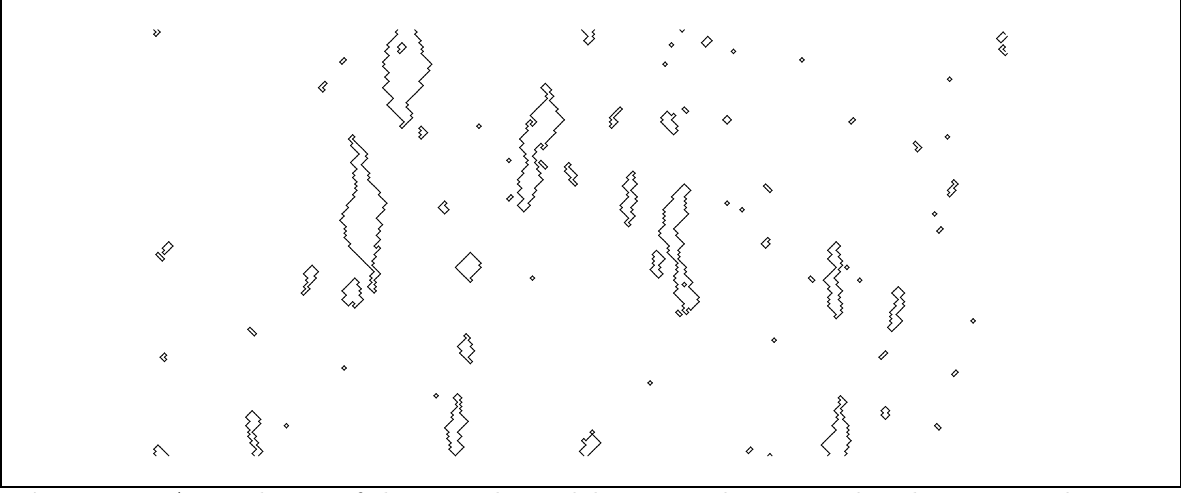


Figure 10: A simulation of the particle model on a 100 by 100 grid with $u = u_i$ and $x = 0.1$ made using Glauber dynamics.

Lemma 14. For $m, n \geq 0$,

$$(6.2) \quad H(m, n) = -\frac{(-1)^{m+n}(1-x)^m(1+x)^n(1+\sqrt{1-x^2})^{2+m-n}(1-x^2+\sqrt{1-x^2})^{-m+n}}{4x^3}$$

Proof. We only prove the result for $m \geq n$. To simplify calculations, set x to $\sqrt{2r+1}/r$. Computing the first integral via residue calculus gives

$$(6.3) \quad \frac{1}{2\pi i} \int_{|w|=1} \frac{r(-1+2r)w^{-n}(w-rw)^m}{2(-1+r+2rw)^m(-1+r+2rw-w^2+rw^2)} dw$$

The singularities of the integrand inside the region $|w| = 1$ are located at $w = (-r + \sqrt{2r-1})/(-1+r)$ and $w = (1-r)/(2r)$. The contribution from the residue at $w = (-r + \sqrt{2r-1})/(-1+r)$ is given by

$$(6.4) \quad \frac{1}{4}r\sqrt{2r-1} \left(\frac{r + \sqrt{2r-1}}{1-r} \right)^{m+n}$$

It remains to find the residue for (6.3) at $w = (1-r)/(2r)$. This can be achieved by splitting the term $(-1+r+2rw-w^2+rw^2) = (r-1)(w-c_1)(w-c_2)$, where $c_1 = 1/c_2$ and $|c_1| < 1$. Hence, the denominator in (6.3) can be separated into

$$(6.5) \quad \frac{1}{(-1+r+2rw-w^2+rw^2)} = \frac{1}{2\sqrt{2r-1}} \left(\frac{1}{w-c_1} - \frac{1}{w-c_2} \right)$$

Each term can then be computed using the high dimensional residue formula:

$$(6.6) \quad \frac{1}{2\pi i} \int_{|w+\frac{1}{2}\frac{1-r}{2r}|=\epsilon} \frac{r\sqrt{2r-1}w^{m-n}(1-r)^m}{2(-1+r+2rw)^m(w-c_1)} = -\frac{1}{4}r\sqrt{2r-1} \left(\frac{r + \sqrt{2r-1}}{1-r} \right)^{m+n}$$

and

$$(6.7) \quad -\frac{1}{2\pi i} \int_{|w+\frac{1}{2}\frac{1-r}{2r}|=\epsilon} \frac{r\sqrt{2r-1}w^{m-n}(1-r)^m}{2(-1+r+2rw)^m(w-c_2)} = \frac{1}{4}r\sqrt{2r-1} \left(\frac{r - \sqrt{2r-1}}{1-r} \right)^{m+n}$$

Notice that contributions from (6.4), (6.6) and (6.7) sum up to give (6.3). As the contributions from (6.4) and (6.6) cancel out, then

$$(6.8) \quad H(m, n) = \frac{1}{4} r \sqrt{2r-1} \left(\frac{r - \sqrt{2r-1}}{1-r} \right)^{m+n}$$

Setting $r = (1 + \sqrt{1-x^2})/x^2$ gives the result. \square

Lemma 14 is an exact result. As a consequence, we can compute the entries of $K^{-1}(v_i, v_j(n, -n))$ exactly. In fact, it turns out that $K^{-1}(v_3, v_3(n, -n)) = K^{-1}(v_3, v_4(n, -n))$ for $u = \frac{1-\sqrt{1-x^2}}{x^2}$. This leads to an interpretation that particle locations are Bernoulli $(\frac{x}{1+x})$, which is argued after the following proposition.

Proposition 6. For $n \geq 1$,

$$(6.9) \quad \mathbb{P}(X(0, t), X(n, t)) = \frac{x^2}{(1+x)^2}$$

Proof. We can calculate the joint probability via the inclusion-exclusion formula given in Lemma 3. Hence, we require

$$(6.10) \quad \text{Pf} \begin{pmatrix} 0 & 1 - xK^{-1}(v_3, v_4) & -K^{-1}(v_3, v_3(n, -n)) & -K^{-1}(v_3, v_4(n, -n)) \\ \cdots & 0 & -K^{-1}(v_4, v_3(n, -n)) & -K^{-1}(v_4, v_4(n, -n)) \\ \cdots & \cdots & 0 & 1 - xK^{-1}(v_3, v_4) \\ \cdots & \cdots & \cdots & 0 \end{pmatrix}$$

where v_i for $i \in \{1, \dots, 6\}$ represents a vertex i in the fundamental domain and $v_i(m, n)$ represents vertex i a distance (m, n) from the fundamental domain.

Using residue calculations, $K^{-1}(v_3, v_4) = 1/(x(x+1))$. It remains to calculate the interaction between the two edges, which can be found by invoking Lemma 14. Due to $K^{-1}(v_3, v_3(n, -n)) = -K^{-1}(v_3, v_4(n, -n))$ for $u = \frac{1-\sqrt{1-x^2}}{x^2}$, by symmetry (6.10) becomes

$$(6.11) \quad \text{Pf} \begin{pmatrix} 0 & 1 - xK^{-1}(v_3, v_4) & 0 & 0 \\ \cdots & 0 & -K^{-1}(v_4, v_3(n, -n)) & K^{-1}(v_4, v_3(n, -n)) \\ \cdots & \cdots & 0 & 1 - xK^{-1}(v_3, v_4) \\ \cdots & \cdots & \cdots & 0 \end{pmatrix}$$

The Pfaffian of the above matrix represents counting the number of weighted perfect matchings of a graph with four vertices w_1, \dots, w_4 , with the edges weighted by the above matrix. Clearly, we can only have one possible contribution (the edges w_1w_2 and w_3w_4), which gives the desired result. \square

The above method can be generalized to consider the locations of an arbitrary number of particles.

Proposition 7. For $i_1 < \dots < i_n$,

$$(6.12) \quad \mathbb{P}(X(i_1, t), \dots, X(i_n, t)) = \frac{x^n}{(1+x)^n}.$$

Proof. Using the inclusion-exclusion formula given in Lemma 3, we can write $\mathbb{P}(X(i_1, t), \dots, X(i_n, t))$ as a Pfaffian of a matrix with block diagonals given by

$$(6.13) \quad \begin{pmatrix} 0 & 1 - xK^{-1}(v_3, v_4) \\ \cdots & 0 \end{pmatrix}$$

and off-diagonal blocks given by

$$(6.14) \quad \begin{pmatrix} -K^{-1}(v_3, v_3(i_k, -i_k)) & -K^{-1}(v_3, v_4(i_k, -i_k)) \\ -K^{-1}(v_4, v_3(i_k, -i_k)) & -K^{-1}(v_4, v_4(i_k, -i_k)) \end{pmatrix}$$

for $k \in \{1, \dots, n\}$. Using the fact that $-K^{-1}(v_3, v_3(i_k, -i_k)) = K^{-1}(v_4, v_3(i_k, -i_k))$, then by applying the graphical representation of the Pfaffian inductively (described in Proposition 6), we can write

$$(6.15) \quad \mathbb{P}(X(i_1, t), \dots, X(i_n, t)) = (1 - xK^{-1}(v_3, v_4))^n.$$

which gives the required result. \square

The locations of the particles are independent and Bernoulli($\frac{x}{1+x}$). It now remains to look at the dynamics.

Proposition 8. *For an arbitrary horizontal line, dimers over the \mathbf{b} edges are iid with distribution Bernoulli($(1/2 - \frac{\sqrt{1-x}}{2\sqrt{1+x}})$).*

Proof. We consider an arbitrary horizontal line. Suppose that L_i represents the event that a dimer covers a \mathbf{b} edge going left (i.e. from v_5 to v_1) where i represents the position of v_4 on the horizontal axis. Let R_i denote the event that a dimer covers a \mathbf{b} edge going right (i.e. from v_6 to v_1) where i represents the position on the lattice v_4 on the horizontal axis.

We first consider the probability of two left going \mathbf{b} edges a distance n away. Without loss of generality, we can consider one of these edges to be located at the origin.

$$(6.16) \quad \mathbb{P}(L_0, L_n) = u^2 x^2 \text{Pf} \begin{pmatrix} 0 & K^{-1}(v_5, v_2(1, 0)) & K^{-1}(v_5, v_5(n, -n)) & K^{-1}(v_5, v_2(1-n, n)) \\ \cdots & 0 & K^{-1}(v_2, v_5) & K^{-1}(v_2, v_5) \\ \cdots & \cdots & 0 & K^{-1}(v_5, v_2(0, 1)) \\ \cdots & \cdots & \cdots & 0 \end{pmatrix}$$

where we have used ‘ \cdots ’ to denote the lower triangle entries (the matrix is anti-symmetric). Then, explicit calculation using Lemma 14 gives

$$(6.17) \quad K^{-1}(v_5, v_5(n, -n)) = K^{-1}(v_5, v_2(n, 1-n))$$

Therefore, using row and column operations on the above matrix gives

$$\begin{aligned} \mathbb{P}(L_0, L_n) &= u^2 x^2 (K_{0,1}^{-1}(5, 2))^2 \\ &= \frac{1 - \sqrt{1-x^2}}{2(1+x)} \end{aligned}$$

A similar result for $\mathbb{P}(R_0, R_n)$ is true, but is reliant on

$$(6.18) \quad K^{-1}(v_6, v_6(n, -n)) = K^{-1}(v_6, v_1(n+1, -n)).$$

The above calculation can be generalized to find the joint probabilities of observing dimers covering any collection of rightward and leftward \mathbf{b} edges located on the same horizontal line. Again, this joint probability is just the product of the probabilities of observing a dimer covering each edge. Furthermore, we can show that the probability of observing n creations along a horizontal line, is given by the product of the probabilities of dimer covering each edge. For example,

$$(6.19) \quad \mathbb{P}(L_0, R_0, L_n, R_n) = u^4 x^4 (K^{-1}(v_5, v_2(0, 1)))^2 (K^{-1}(v_6, v_1(0, 1)))^2$$

□

A further calculation shows that the trajectories of particles are independent. This relies on computing the possible trajectories of the particles given their locations. This calculation follows in the same vein as the previous propositions.

Proof of Theorem 3. For $u = \frac{1-\sqrt{1-x^2}}{x^2}$, the dimer covering of the Fisher lattice can be thought as follows:

- Take an arbitrary horizontal line along the **a** edges. With product measure, we can place dimers on **a** edges with an iid Bernoulli ($\frac{1}{1+x}$) distribution.
- If there is no dimer covering an **a** edge on the row below (or above), then choose a dimer to cover either the left or right **b** edge directly above (or below) with probability $\frac{1}{2}$. This is a direct consequence of seeing one **b** edge conditioned on there not being a **b** edge on the row below (above). The surrounding dimers are automatically selected from this probabilistic choice.
- If there is a dimer covering **a** edge on the row below, then with probability $(1 - \sqrt{1-x^2})/(2+2x)$, select two dimers to cover both directly above (below) **b** edges. Otherwise, cover the edge v_5 to v_6 with a dimer.

As a consequence of locating all the dimers on the **b** edge row, determines the existence of dimer on the above (below) **a** edges row.

Due to the independence of the entries, the model can be viewed as a one dimensional noisy voter model with two colors, say red and blue. The particles in the dimer model represent the boundary between the two colors. A site contained within a connected region of the same color can flip color with Bernoulli $(1 - \sqrt{1-x^2})/(2+2x)$. This represents the noise. Hence, the particle model is in direct correspondence with the noisy voter model. The scaling window (x, x^2) of the noisy voter model was constructed in [FINR06] and named the Continuum Noisy Voter model.

□

An equivalent interpretation of this dimer model is a one-dimensional Ising Model with heat bath dynamics. This can be seen via the two-dimensional Ising model representation of the dimer model. The fact that there are no correlations amongst the spins along any horizontal line of the Ising model in two dimensions implies that the interaction of the spins is only dependent on the previous levels.

6.2. Creation Measure. Similar to $u = u_c$, the set of creations for the case $u = u_i$ forms a dense set in the scaling window (x, x^2) . However, we can restrict to the set of creations which give paths of length greater than ϵ in the scaling window. This section shows that this random set is finite and its points form a Poisson point process.

We use the same notation as Section 5.3 without further mention.

Lemma 15.

$$(6.20) \quad 0 < \lim_{x \rightarrow 0} \mathbb{E} |\Gamma_B^\epsilon| < \infty$$

Proof. The proof of the upper bound follows by the same argument given in Lemma 12.

For the lower bound, define $X_t(y, z) = P_r(y, z, t - z) - P_l(y, z, t - z)$ for $(y, z) \in \Xi_B$. This means $\{X_t(y, z) : (y, z) \in \Xi_B\}$ is a set of independent walks with i.i.d. increments of 1 with

probability 1/4, 0 with probability 1/2 and -1 with probability 1/4. Let X_t represent one copy of these walks. Then, using the same arguments of Lemma 12,

$$(6.21) \quad \lim_{x \rightarrow 0} \mathbb{E}[|\Gamma_B^\epsilon|] = \lim_{x \rightarrow 0} \mathbb{E}[|\Xi_B|] \mathbb{P}_1(T_0^X > \epsilon/x^2)$$

$\mathbb{P}_1(T_0^X > \epsilon/x^2)$ has already been computed in Lemma 12 and is $\Theta(x)$. $\mathbb{E}[|\Xi_B|]$ is $1/x^3$ multiplied by the expected number of creations in a fundamental domain. Therefore, $\mathbb{E}[|\Xi_B|] = c/x + O(1)$. Hence,

$$(6.22) \quad \lim_{x \rightarrow 0} \mathbb{E}[|\Gamma_B^\epsilon|] > 0$$

□

As in Section 5.3, $\mathbb{E}[|\Gamma_B^\epsilon|]$ is dependent on ϵ . Moreover, $\lim_{\epsilon \rightarrow 0} \mathbb{E}[|\Gamma_B^\epsilon|] = \infty$.

Theorem 7. $\mathbb{P}_{x,\epsilon}^{s,u_i}$ converges weakly to a Poisson point process as $x \rightarrow 0$.

Proof. By using Lemma 14, then it can be shown that the creation singularities are independent. In other words, the statement Lemma 13 can be replaced by

$$(6.23) \quad \mathbb{P}(X = y_1, \dots, X = y_k) = \prod_{i=1}^k \mathbb{P}(X = y_i)$$

for $k > 0$ and $y_1, \dots, y_k \in B$. Following the proof of Theorem 6, using the above equation where necessary gives the required result. □

Remark: Let $P_l^\epsilon = \{P_l(z, y) : (z, y) \in \Gamma_B^\epsilon\}$ and define P_r^ϵ accordingly. Let $\mathbb{P}_{0,\epsilon}^{sing}$ denote the limiting Poisson point process for $P_{x,\epsilon}^{sing}$ with $\epsilon > 0$ fixed. Then, define $R(\epsilon) = \{\mathbb{P}_{0,\epsilon}^{sing}, P_l^\epsilon, P_r^\epsilon\}$ denotes the CNVM conditioned on having path lengths of at least $\epsilon > 0$.

7. THE SCALING AROUND u_c AND u_i

This section concentrates on the behavior exhibited when $u = (1 - \sqrt{1 - \gamma x^2})/(\gamma x^2)$ with $\gamma \in \mathbb{R} \setminus \{-1, 1\}$ and $|\gamma| = o(1/x)$ (i.e. $u = 1/2 - \gamma x^2/8$). We find the stationary measure for the locations of particles on a horizontal line for the scaling window (x, x^2) . There are three cases to be considered, namely, $\gamma < -1$, $\gamma \in (-1, 1)$ and $\gamma > 1$. These correspond to $u < u_c$, $u_c < u < u_i$ and $u > u_i$. For each case, particle locations are given by a Pfaffian point process. However, each process exhibits different local behaviors, which are discussed after the following lemma.

Lemma 16. Suppose that $nx = \alpha$ where $\alpha \in [0, \infty)$ and $\gamma \in \mathbb{R} \setminus \{-1, 1\}$. Then

$$(7.1) \quad K^{-1}(v_3, v_3(n, -n)) = E_1^\gamma(\alpha) + O(x)$$

and

$$(7.2) \quad K^{-1}(v_3, v_4(n, -n)) = E_2^\gamma(\alpha) + O(x)$$

where

$$(7.3) \quad E_1^\gamma(\alpha) = -\frac{1}{\pi i} \int_{e_2(\gamma)}^{e_1(\gamma)} \frac{2pe^{-\alpha p}}{\sqrt{4 + 8\gamma + 4\gamma^2 - 12p^2 + 4\gamma p^2 + p^4}} dp + O(x)$$

and

$$(7.4) \quad E_2^\gamma(\alpha) = \frac{1}{\pi i} \int_{e_2(\gamma)}^{e_1(\gamma)} \frac{(-2 - 2\gamma - p^2)e^{-\alpha p}}{2\sqrt{4 + 8\gamma + 4\gamma^2 - 12p^2 + 4\gamma p^2 + p^4}} dp + O(x)$$

where $e_1(\gamma) = 2 + \sqrt{2(1-\gamma)}$ and $e_2(\gamma) = (2 - \sqrt{2(1-\gamma)})\mathbb{I}_{\gamma > -1} + (-2 + \sqrt{2(1-\gamma)})\mathbb{I}_{\gamma < -1}$.

Lemma 16 provides the inverse Kastelyn entries, which can be used to compute correlations. For $\gamma > 1$, notice that $e_1(\gamma) = e_2(\gamma)$. For $\gamma < 1$, it can be shown that $|E_1^\gamma(\alpha)| > |E_2^\gamma(\alpha)|$. This implies that any pair of particles is positively correlated. However, for $\gamma > 1$, it can be shown that $|E_1^\gamma(\alpha)| < |E_2^\gamma(\alpha)|$, which shows that any pair of particles is negatively correlated.

Lemma 16 is also valid for $\gamma = -1$ but not for $\gamma = 1$. From the observation that $e_2(-1) = 0$, then clearly the decay of $E_1^{-1}(\alpha)$ in the limit $\alpha \rightarrow 0$ is slower than the decay of $E_1^\gamma(\alpha)$ in the limit $\alpha \rightarrow 0$ for other $\gamma \notin \{-1, 1\}$. This results in the covariance to decay slower in distance at u_c , then any other value of u .

The entry for $K^{-1}(v_3, v_4)$ can also be computed up to $O(x)$ in a similar fashion as the other entries in Lemma 16. Let $e(\gamma) = \lim_{x \rightarrow 0} 1/x(1 - xK^{-1}(v_3, v_4))$. Then,

$$(7.5) \quad e(\gamma) = \lim_{x \rightarrow 0} \frac{1}{x} (1 - xK^{-1}(v_3, v_4)) = \frac{1}{\pi i} \int_{e_2(\gamma)}^{e_1(\gamma)} \frac{2 - 2\gamma + p^2}{2\sqrt{4 + 8\gamma + 4\gamma^2 - 12p^2 + 4\gamma p^2 + p^4}} dp$$

Under the scaling window (x, x^2) and the limit $x \rightarrow 0$, the particle locations are given by Theorem 4. We can now prove Theorem 4

Proof of Theorem 4. The structure of the matrix comes from Lemma 3. The relevant entries come from Lemma 16. The proof of weak convergence is the same as the proof in Theorem 4 for $u = u_c$. \square

It remains to compute the inverse Kastelyn entries. Let

$$(7.6) \quad \tilde{P}(z, w) = zwP(z, w) = zw \det K(z, w)$$

Proof of Lemma 16. For the sake of brevity, we only compute $K^{-1}(v_3, v_3(n, -n))$. The entry is given by

$$(7.7) \quad K^{-1}(v_3, v_3(n, -n)) = \frac{1}{(2\pi i)^2} \int_{\mathbb{T}^2} \frac{-u^2(w^{-n+1}z^{n-1} - w^{-n-1}z^{n+1})}{\tilde{P}(z, w)} dz dw$$

Taking the transformation $z = \zeta w$ gives

$$(7.8) \quad K^{-1}(v_3, v_3(n, -n)) = \frac{1}{(2\pi i)^2} \int_{\mathbb{T}^2} \frac{(u^2 \zeta^{n-1} (\zeta^2 - 1))}{\tilde{P}(\zeta w, w)} dw d\zeta.$$

As $\tilde{P}(\zeta w, w) = C(w - w_1)(w - w_2)$ where C, w_1 and w_2 are rational functions of ζ , with $|w_1| > 1$ and $|w_2| < 1$ then computing the integral with respect to w via residue calculus gives

$$(7.9) \quad K^{-1}(v_3, v_3(n, -n)) = \frac{1}{2\pi i} \int_{|\zeta|=1} \frac{(u^2 \zeta^{n-1} (\zeta^2 - 1))}{\sqrt{A(\zeta)}} d\zeta$$

where

$$(7.10) \quad A(\zeta) = (w_1 - w_2)u\zeta(1 + \zeta)(-1 + u^2\zeta^2)$$

Recalling the expressions $e_1(\gamma)$ and $e_2(\gamma)$ and denote $e_3(\gamma) = 3 - \gamma + 2\sqrt{2(1-\gamma)}$ and $e_4(\gamma) = 3 - \gamma - 2\sqrt{2(1-\gamma)}$. Then, $A(\zeta)$ can be factorized into the following

$$(7.11) \quad A(\zeta) = u^4(-1+x^2)^2(\zeta - (1+e_1x+e_3x^2))(\zeta - (1+e_2x+e_4x^2))(\zeta - (1-e_1x+e_3x^2))(\zeta - (1-e_2x+e_4x^2)) + O(x^3)$$

Taking the change of variables $\zeta = 1 - x\xi$ transforms $A(\zeta)$ in (7.11) into the following
(7.12)

$$A(\xi) = x^4 u^4 (-1 + x^2)^2 ((\xi - (e_1 + e_3 x))(\xi - (e_2 + e_4 x))(\xi - (e_1 + e_3 x))(\xi - (e_2 + e_4 x)) + O(x^2))$$

while (7.9) becomes

$$(7.13) \quad K^{-1}(v_3, v_3(n, -n)) = \frac{1}{2\pi i} \int_{|\xi-1/x|=1/x} \frac{xu^2(1-x\xi)^{n-1}((1-x\xi)^2-1)}{\sqrt{A(\xi)}} d\xi$$

The contour of integration can be pushed to a contour independent of x surrounding the two roots of $A(\xi)$ with positive real part, namely a contour surrounding $e_1(\gamma)$ and $e_2(\gamma)$. Notice that $e_1(\gamma)$ and $e_2(\gamma)$ are defined so that we can keep track of the roots with positive real part. Then, the numerator of the above integrand tends to

$$(7.14) \quad \frac{1}{2} e^{-\alpha\xi} \xi x^2$$

as $x \rightarrow 0$ whereas the denominator tends to

$$(7.15) \quad -\frac{1}{4} x^2 \sqrt{4 + 8\gamma + 4\gamma^2 - 12\xi^2 + 4\gamma\xi^2 + \xi^4}$$

By the denominated convergence theorem, we obtain

$$(7.16) \quad K^{-1}(v_3, v_3(n, -n)) = -\frac{1}{2\pi i} \int \frac{2e^{-\alpha\xi} \xi}{\sqrt{4 + 8\gamma + 4\gamma^2 - 12\xi^2 + 4\gamma\xi^2 + \xi^4}} d\xi.$$

where the integral is over a contour surrounding $e_1(\gamma)$ and $e_2(\gamma)$. Splitting up the contour into two line integrals gives the required result. \square

Although Lemma 16 incorporates Lemma 11, the technique used to calculate Lemma 11 is more general. Moreover, we can use the same technique found in Lemma 11 when the indices of z and w are different. This is required in Lemma 13. The calculation for Lemma 16 cannot be generalized in this way.

7.1. Correlation Length. This subsection focuses on proving Lemma 1.16. Recall that the correlation length, $\xi(\gamma)$ (1.16) is defined in terms $C(\alpha, \gamma) = E_1^\gamma(\alpha)^2 - E_2^\gamma(\alpha)^2$ for $\gamma \neq 1$ and $C(\alpha, 1) = 0$ for all $\alpha \geq 0$.

Proof of Lemma 1.16. We split the proof into the various cases.

For $\gamma = 1$, $C(\alpha, 1) = 0$ for all $\alpha \geq 0$, which implies that $\xi(1) = 0$. As $C(\alpha, -1) \sim 1/\alpha^2$, then $\xi(-1) = \infty$.

For $-1 < \gamma < 1$, we can set up bounds for $E_1^\gamma(\alpha)$ and $E_2^\gamma(\alpha)$ for α large:

$$(7.17) \quad e^{-\alpha e_1(\gamma)} E_1^\gamma(0) \leq E_1^\gamma(\alpha) \leq e^{-\alpha e_2(\gamma)} E_1^\gamma(0)$$

and similarly

$$(7.18) \quad e^{-\alpha e_1(\gamma)} E_2^\gamma(0) \leq E_2^\gamma(\alpha) \leq e^{-\alpha e_2(\gamma)} E_2^\gamma(0)$$

Therefore,

$$(7.19) \quad e^{-2\alpha e_1(\gamma)} E_1^\gamma(0)^2 - e^{-2\alpha e_2(\gamma)} E_2^\gamma(0)^2 \leq C(\alpha, \gamma) \leq e^{-2\alpha e_2(\gamma)} E_1^\gamma(0)^2 - e^{-2\alpha e_1(\gamma)} E_2^\gamma(0)^2.$$

Using these bounds in the definition of $\xi(\gamma)$ gives

$$(7.20) \quad \frac{1}{2e_2(\gamma)} \leq \xi(\gamma) \leq \frac{1}{2e_1(\gamma)}$$

as required.

For $\gamma < -1$, (7.17) still holds but (7.18) does not necessarily hold. Split $E_2^\gamma(\alpha)$ into its positive and negative parts, i.e.

$$(7.21) \quad E_2^\gamma(\alpha) = (E_2^\gamma(\alpha))_+ - (E_2^\gamma(\alpha))_-,$$

with $(E_2^\gamma(\alpha))_+$ having bounds of integration $e_2(\gamma)$ up to $\sqrt{2(-\gamma-1)}$ and $(E_2^\gamma(\alpha))_-$ having bounds of integration $\sqrt{2(-\gamma-1)}$ up to $e_1(\gamma)$. Then,

$$(7.22) \quad |E_2^\gamma(\alpha)| \leq e^{-e_2(\gamma)\alpha} (E_2^\gamma(0))_+.$$

and

$$(7.23) \quad |E_2^\gamma(\alpha)| \geq e^{-\sqrt{2(-\gamma-1)}\alpha} (E_2^\gamma(0))_+ + e^{-e_1(\gamma)\alpha} (E_2^\gamma(\alpha))_-$$

Plugging these bounds into $C(\alpha, \gamma)$ and using the definition of $\xi(\alpha, \gamma)$ gives the required result.

For $\gamma > 1$, the underlying integrals are contour integrals, with the contour having constant real part. From the definition of $C(\alpha, \gamma)$, we can consider $|E_1^\gamma(\alpha) - E_2^\gamma(\alpha)|$ and $|E_1^\gamma(\alpha) - E_2^\gamma(\alpha)|$ separately. For notational convenience, set $r = \sqrt{2(\gamma-1)}$. By applying the change of variables $p \mapsto 2 + ip$ then

$$(7.24) \quad |E_1^\gamma(\alpha) - E_2^\gamma(\alpha)| = 2 \frac{e^{-2\alpha}}{\pi} \operatorname{Re} \int_0^r \sqrt{\frac{(p-r)(p+r)}{(p-2i+r)(p-2i+r)}} e^{-i\alpha p} dp$$

and

$$(7.25) \quad |E_1^\gamma(\alpha) - E_2^\gamma(\alpha)| = 2 \frac{e^{-2\alpha}}{\pi} \operatorname{Re} \int_{-r}^r \sqrt{\frac{(p-2i+r)(p-2i+r)}{(p-r)(p+r)}} e^{-i\alpha p} dp$$

by splitting up the domain of integration into two parts $(-r, 0)$ and $(0, r)$. The integral in (7.24) decays at rate $1/r$. This can be seen by applying integration by parts and integrating the term $\sqrt{p-r} e^{-i\alpha p}$. Employing a similar technique shows that (7.25) decays at rate $1/\sqrt{r}$. Therefore,

$$(7.26) \quad \lim_{\alpha \rightarrow \infty} \frac{1}{\alpha} \log C(\alpha, \gamma) = -\frac{1}{4}.$$

Plugging back into the definition of the correlation length gives the result. \square

We conclude with some remarks about the correlation length. Choosing $\gamma = 1 + Cx^a$, where $C > 0$ and $a > 0$, forces the covariance between particles to converge to 0 in the scaling window (x, x^2) . This can be shown either using an analogous calculation (7.17), or by using an expansion of the covariance around $u = u_i$. As $\lim_{\gamma \rightarrow 1^+} \xi(\gamma) = 1/4$, $\lim_{\gamma \rightarrow 1^-} \xi(\gamma) = 1/4$ and $\xi(1) = 0$, then there is a point of discontinuity for the correlation length at $\gamma = 1$. This is a consequence of the definition of the correlation length as opposed to a difference of measures. This can be seen by setting $u = u_i + \epsilon x^2$ and showing that all the finite distributions converge (after taking the scaling window) in the limit $\epsilon \rightarrow 0$.

8. CONCLUDING REMARKS

Here, we describe some possibilities for future work that we have been unable to complete so far.

As noted before, we have been unable to find the limiting measure for the scaling window (x, x^2) when $u = (1 - \sqrt{1 - \gamma x^2})/(\gamma x^2)$ for $\gamma \neq 1$. When $\gamma = -1$, we expect that this limiting measure is scale invariant but not rotationally invariant. This is due to the underlying dimer model (or Ising model) being anisotropic. The techniques used in this paper have primarily concentrated on spin-spin correlations. In the same way that the scaling limit of percolation (see [CN06]) required SLE and CLE (see [Wer04] or [Law05] for fine surveys of SLE), we expect that the scaling windows of this Ising Model requires some family of random curves and loops.

Taking $x = 1$ in the underlying dimer model forces the coefficient of z/w and w/z in the characteristic polynomial to be zero. For $u = 1$, $P(z, w)$ is a constant. This implies that spins from the Ising Model are chosen independently with probability $1/2$, which is exactly percolation on the triangular lattice. For $u < 1$, the inverse Kastelyn entries can be written in terms of the Green's function for random walks on the triangular lattice. Choosing $u = \sqrt{2} - 1$, the Green's function is the inverse of the Laplacian.

If we take $u = u_i + \epsilon^2$ where ϵ is order x^α for $\alpha \in (0, 1)$, then

$$(8.1) \quad \mathbb{E}[N_b] = \mathbb{E}[N_a] + O(x) = O(\epsilon)$$

and

$$(8.2) \quad \mathbb{E}[N_X] = x^2 + \epsilon O(x^2 \log x).$$

These can be shown by expanding out the appropriate elliptic integrals defined in Section 3. By taking the scaling window $(x^\alpha, x^{2\alpha})$ implies that the density of particles is of constant order. For $\alpha < 2/3$, there is a dense set of creations in the scaling window. For $\alpha > 2/3$, then there are no creations or annihilations seen in the scaling window $(x^\alpha, x^{2\alpha})$. We expect the limiting measure to be Dyson Brownian motions. For $\alpha = 2/3$, the creations have a finite density. Roughly speaking, we expect the repulsion of the particles to be weak enough to allow some annihilations.

Finally, is there a random matrix ensemble, whose eigenvalues have the same distribution as the particle locations in the scaling limit for $u = u_c$? This question is motivated from the fact that dimer coverings on the honeycomb lattice are a 'discretized' version of a GUE.

REFERENCES

- [AB99] M. Aizenman and A. Burchard. Hölder regularity and dimension bounds for random curves. *Duke Math. J.*, 99(3):419–453, 1999.
- [Arr79] R.A. Arratia. *Brownian Motions on the line*. PhD thesis, University of Wisconsin, Madison, 1979.
- [BdT08] Cedric Boutillier and Beatrice de Tiliere. The critical z-invariant ising model via dimers: the periodic case, 2008.
- [Bou07] C. Boutillier. Non-colliding paths in the honeycomb dimer model and the dyson process. *Journal of Statistical Physics*, 129:1117–1135, 2007.
- [Cam08] Federico Camia. Scaling limits of two-dimensional percolation: an overview. *Statistica Neerlandica*, 62(3):314–330, 2008.
- [CCFS89] J. T. Chayes, L. Chayes, Daniel S. Fisher, and T. Spencer. Correlation length bounds for disordered Ising ferromagnets. *Comm. Math. Phys.*, 120(3):501–523, 1989.
- [Chh11] S. Chhita. *Scaling Windows for Dimer models*. PhD thesis, Brown University, 2011.
- [CN06] Federico Camia and Charles M. Newman. Two-dimensional critical percolation: the full scaling limit. *Comm. Math. Phys.*, 268(1):1–38, 2006.

- [DVJ88] D. J. Daley and D. Vere-Jones. *An introduction to the theory of point processes*. Springer Series in Statistics. Springer-Verlag, New York, 1988.
- [FFS92] Roberto Fernández, Jürg Fröhlich, and Alan D. Sokal. *Random walks, critical phenomena, and triviality in quantum field theory*. Texts and Monographs in Physics. Springer-Verlag, Berlin, 1992.
- [FINR04] L. R. G. Fontes, M. Isopi, C. M. Newman, and K. Ravishankar. The Brownian web: characterization and convergence. *Ann. Probab.*, 32(4):2857–2883, 2004.
- [FINR06] L. R. G. Fontes, M. Isopi, C. M. Newman, and K. Ravishankar. Coarsening, nucleation, and the marked Brownian web. *Ann. Inst. H. Poincaré Probab. Statist.*, 42(1):37–60, 2006.
- [Fis66] M.E. Fisher. On the dimer solution of planar ising models. *Journal of Mathematical Physics*, 7:1776–1781, 1966.
- [GM95] Boris L. Granovsky and Neal Madras. The noisy voter model. *Stochastic Process. Appl.*, 55(1):23–43, 1995.
- [God93] C. D. Godsil. *Algebraic combinatorics*. Chapman and Hall Mathematics Series. Chapman & Hall, New York, 1993.
- [Kas61] P.W. Kasteleyn. The statistics of dimers on a lattice: I. the number of dimer arrangements on a quadratic lattice. *Physica*, 27:1209–1225, 1961.
- [Ken97] Richard Kenyon. Local statistics of lattice dimers. *Ann. Inst. H. Poincaré Probab. Statist.*, 33(5):591–618, 1997.
- [Ken00] Richard Kenyon. Conformal invariance of domino tiling. *Ann. Probab.*, 28(2):759–795, 2000.
- [Ken09] Richard Kenyon. Lectures on dimers. In *Statistical mechanics*, volume 16 of *IAS/Park City Math. Ser.*, pages 191–230. Amer. Math. Soc., Providence, RI, 2009.
- [KOS06] Richard Kenyon, Andrei Okounkov, and Scott Sheffield. Dimers and amoebae. *Ann. of Math. (2)*, 163(3):1019–1056, 2006.
- [Law89] Derek F. Lawden. *Elliptic functions and applications*, volume 80 of *Applied Mathematical Sciences*. Springer-Verlag, New York, 1989.
- [Law05] Gregory F. Lawler. *Conformally invariant processes in the plane*, volume 114 of *Mathematical Surveys and Monographs*. American Mathematical Society, Providence, RI, 2005.
- [Lig85] Thomas M. Liggett. *Interacting particle systems*, volume 276 of *Grundlehren der Mathematischen Wissenschaften [Fundamental Principles of Mathematical Sciences]*. Springer-Verlag, New York, 1985.
- [Sch00] Oded Schramm. Scaling limits of loop-erased random walks and uniform spanning trees. *Israel J. Math.*, 118:221–288, 2000.
- [She05] Scott Sheffield. Random surfaces. *Astérisque*, (304):vi+175, 2005.
- [Sos00] A. Soshnikov. Determinantal random point fields. *Uspekhi Mat. Nauk*, 55(5(335)):107–160, 2000.
- [Wer04] Wendelin Werner. *Random planar curves and Schramm-Loewner evolutions*, volume 1840 of *Lecture Notes in Math*. Springer, Berlin, 2004.

BROWN UNIVERSITY, PROVIDENCE, RI, USA
 E-mail address: `schhita@math.brown.edu`